Post-transcriptional control of C/EBPα and C/EBPβ proteins

Zaini, Mohamad Amr

3

CHAPTER III

A p300 and SIRT1 regulated acetylation switch of C/EBPα controls mitochondrial function

Mohamad Amr Zaini[1,2], Christine Müller[1], Tristan de Jong[1], Tobias Ackermann[1], Götz Hartleben[1], Gertrud Kortman[1], Karl-Heinz Gührs[2], Fabrizia Fusetti[3], Oliver H. Krämer[4], Victor Guryev[1] and Cornelis F Calkhoven[1].

[1]European Research Institute for the Biology of Ageing (ERIBA), University Medical Center Groningen, the Netherlands. [2]Leibniz Institute for Age Research - Fritz Lipmann Institute, Jena, Germany. [3]University of Groningen, Groningen, The Netherlands.[4]Institute of Toxicology, University Medical Center Mainz, Mainz, Germany.

Manuscript revised and resubmitted to Cell reports journal

Abstract

Cellular metabolism is a tightly controlled process in which the cell adapts fluxes through metabolic pathways in response to changes in nutrient supply. Among the transcription factors that regulate gene expression and thereby cause changes in cellular metabolism is the basic leucine-zipper (bZIP) transcription factor CCAAT/enhancer-binding protein alpha (C/EBPα). Protein lysine acetylation is a key post-translational modification (PTM) that integrates cellular metabolic cues with other physiological processes. Here we show that C/EBPα is acetylated by the lysine acetyl transferase (KAT) p300 and deacetylated by the lysine deacetylase (KDAC) Sirtuin1 (SIRT1). SIRT1 is activated in times of energy demand by high levels of nicotinamide adenine dinucleotide (NAD^+) and controls mitochondrial biogenesis and function. A non-acetylated mutant of C/EBPα induces the transcription of mitochondrial genes and results in increased mitochondrial respiration. Our study identifies C/EBPα as a key mediator of SIRT1-controlled adaption of energy homeostasis to changes in nutrient supply.

Introduction

Studies in cell culture and with mouse models have demonstrated a key role for C/EBPα in regulating the transcription of metabolic genes. C/EBPα deficiency in mice results in severe metabolic phenotypes, particularly affecting the liver tissue structure and its functions in gluconeogenesis, glycogen synthesis and bilirubin clearance as well as its deficiency affects fat storage in white adipose tissue (WAT) [1-6]. In addition, C/EBPα together with PPARγ are key factors in the transcriptional network controlling adipocyte differentiation [7-9], and mutations of phosphorylation sites in regulatory domains of C/EBPα results in dysregulated transcription of genes involved in glucose and lipid metabolism *in vivo* [7,10]. Hence, C/EBPα is a key factor for the differentiation and function of hepatocytes and adipocytes and plays an essential role in the regulation of energy homeostasis.

Protein lysine acetylation is a key post-translational modification (PTM) that integrates cellular metabolic cues with other physiological processes, including cell growth and proliferation, circadian rhythm and energy homeostasis [11-13]. Acetylation may regulate various functions of the acetylated proteins including changes in DNA binding, protein stability, enzymatic activity, protein-protein interactions and subcellular localization. Protein acetylation is a reversible process in which an acetyl group is transferred from an acetyl coenzyme A (acetyl-CoA) to the target lysine residue by lysine acetyl transferases (KATs) and is removed by lysine deacetylases (KDACs). The KATs and KDACs consist of a large group of enzymes originally identified to acetylate histones as part of epigenetic mechanisms. Later also non-histone proteins were identified as KAT targets [11]. Sirtuins (class III KDACs) are lysine deacetylases that require nicotinamide adenine dinucleotide (NAD^+) as co-factor for their enzymatic activity and therefore are activated in times of energy demand when NAD^+ levels are high (high NAD^+/NADH ratio)[14].

Involvement of KATs in C/EBPα mediated transcription has been reported in the past [15-18], however, the role C/EBPα protein lysine acetylation in the transcriptional regulation of metabolic genes has not been addressed. Since C/EBPα is a key regulator of metabolism we hypothesized that reversible acetylation of C/EBPα is decisively involved in regulating metabolic homeostasis. Here we show that C/EBPα is acetylated on lysines K159 and K298 by the KAT p300, which modulates the transcriptional activity of C/EBPα. We show that acetylation of

C/EBPα is dependent on glucose availability and we identify SIRT1 as the sole sirtuin that mediates NAD^+-dependent deacetylation of C/EBPα. A hypoacetylated mutant of C/EBPα induces the expression of genes involved in the function of the mitochondrion and oxidation-reduction processes, which is accompanied by an increase in mitochondrial mass and cellular oxygen consumption rates. Our study shows that reversible acetylation of C/EBPα in response to changed metabolic conditions alters its transcriptional function to adapt metabolic gene expression and plays an important role in SIRT1-controlled cellular metabolic homeostasis.

Results

Acetylation of C/EBPα by p300 enhances its transactivation activity

The presence of fifteen conserved lysines in sequences of vertebrate C/EBPα orthologs suggests that C/EBPα is a potential target for lysine acetylation (**Figure S1A**). Glucose-rich cell culture conditions are known to increase protein-acetylation through increased availability of acetyl-CoA as substrate for KATs to donate an acyl group to the target lysine [19]. Acetylation of endogenous C/EBPα in lysates from the Fao rat hepatoma cell line was detected using an anti-acetylated lysine (anti-Ac-K) antibody following immunoprecipitation (IP) of C/EBPα under high glucose (25 mM) conditions, which was reduced under low glucose (5 mM) conditions (**Figure 1A**). Acetylation of immunoprecipitated C/EBPα was also detected in HEK293T cells lacking endogenous C/EBPα that were transfected with a C/EBPα expression vector (**Figure 1B**). Next we investigated whether co-expression of the four major KATs, p300, P/CAF, GCN5 or Tip60 alter the transcriptional activity of C/EBPα using a luciferase-based reporter solely containing two natural C/EBP-binding sites of the cMGF promoter [20]. Co-transfection with p300 resulted in an increase in C/EBPα-induced promoter activity in a dose dependent manner whereas co-transfection with the other KATs had no significant effect (**Figures 1C, D and S1B**). To investigate a direct interaction between C/EBPα and p300 as well as three additional major KATs we co-expressed C/EBPα with p300-HA, P/CAF-FLAG, GCN5-FLAG or Tip60 in HEK293T cells and performed co-immunoprecipitation experiments using anti-C/EBPα antibodies. C/EBPα co-precipitated with p300, P/CAF, GCN5, but not with

Tip60 (**Figure S1C**), which was confirmed by reciprocal, co-immunoprecipitation of the C/EBPα with the same KATs (**Figures 1E and S1D**). To examine whether the intrinsic KAT function of p300 is involved in C/EBPα acetylation and transactivation potential, we co-expressed C/EBPα with either p300 or p300 with its KAT-domain deleted (p300ΔKAT-HA) and analyzed C/EBPα acetylation and p300 binding by C/EBPα co-immunoprecipitation. C/EBPα acetylation was abolished by expression of p300ΔKAT-HA (**Figure 1F**). In addition, the p300 dependent C/EBPα transactivation activity is abrogated by deletion of the p300-KAT (**Figure 1D**). In addition, p300-mediated acetylation of C/EBPα in HEK293 cells is strongly reduced under low glucose conditions (5 mM), confirming that protein acetylation is facilitated under conditions of high acetyl-CoA availability (**Figure 1G**). Moreover, in Fao cells acetylation of endogenous C/EBPα was abolished by treatment with the p300 inhibitor C646 (**Figure 1H**). Therefore, we propose that p300 catalyzes the acetylation of C/EBPα and thereby alters its transcriptional function.

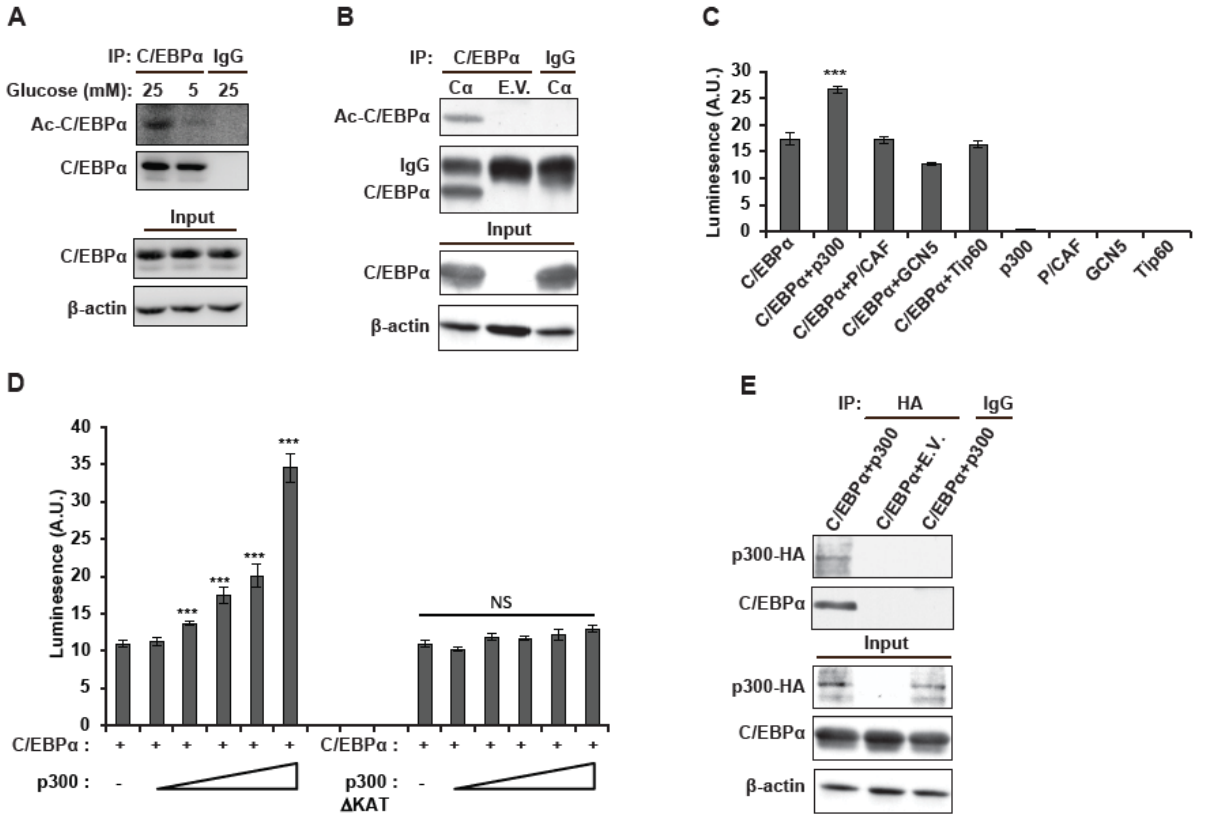

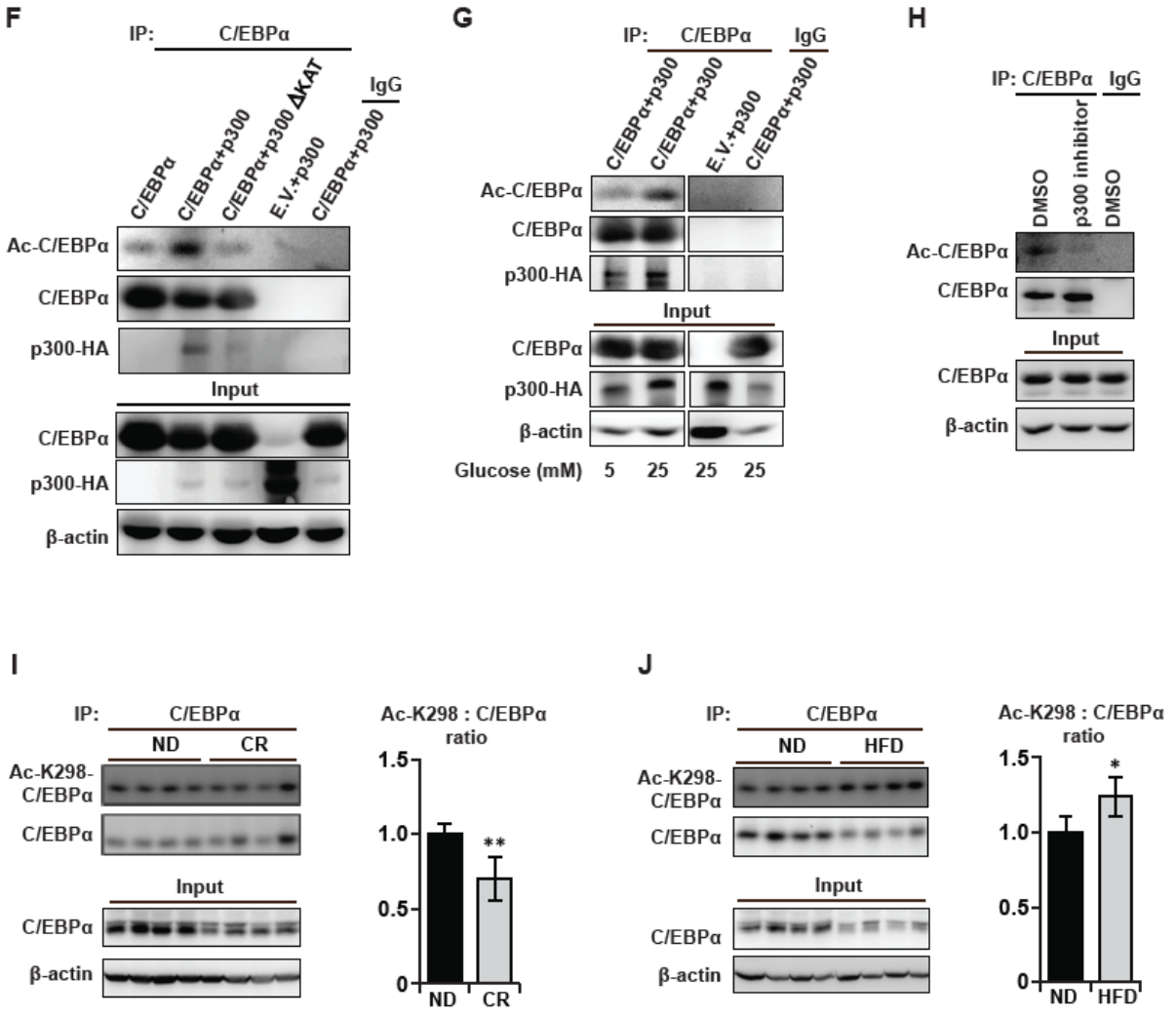

Figure 1. Acetylation of C/EBPα by p300 enhances its transactivation activity.

(**A**) Immunoprecipitation (IP) of endogenous C/EBPα was performed with rabbit anti-C/EBPα antibody or with rabbit IgG as control from total lysates of Fao cells cultured overnight in either high (25 mM) or low (5 mM) glucose medium. The immunoprecipitates (IP) and total lysates (Input) were analyzed by immunoblotting for C/EBPα, acetylated lysine or β-actin loading control as indicated.

(**B**) C/EBPα (Cα) was immunoprecipitated from total lysates of HEK293T cells ectopically expressing C/EBPα or empty vector (E.V.) control. The immunoprecipitates (IP) and total lysates (Input) were analyzed by immunoblotting for C/EBPα, acetylated lysine or β-actin loading control as indicated.

(**C**) HEK293T cells were transiently transfected with C/EBP-responsive firefly-reporter vector, a renilla expression vector for normalization, C/EBPα and/or one of the lysines acetyl transferases (KATs) expressing vector as indicated. Luciferase activity was measured 48 h later (n=4).

(**D**) HEK293T cells were transiently transfected with luciferase C/EBP-responsive firefly-reporter vector, renilla expression vector for normalization, C/EBPα and increased amounts of either wt p300-HA or ΔKATp300-HA (p300 with its lysine acetyl transferase domain deleted) expression vectors. Luciferase activity was measured 48 h later (n=4).

(**E**) HEK293T cells were transiently transfected with C/EBPα and either pcDNA3 empty vector (E.V.) or p300-HA expression vector. Cell lysates were immunoprecipitated with either mouse anti-HA antibody or with mouse IgG as control followed by immunoblotting. Immunoblots of immunoprecipitates (IP) and total lysates (Input) were stained as indicated.

(**F**) HEK293T cells were transiently transfected with C/EBPα and either wt p300-HA or ΔKATp300-HA expression vectors. Cell lysates were immunoprecipitated with either rabbit anti-C/EBPα antibody or with rabbit IgG as control followed by immunoblotting. Immunoblots of immunoprecipitates (IP) and total lysates (Input) were stained as indicated.
(**G**) HEK293T cells were transiently transfected with p300-HA and either pcDNA3 empty vector (E.V.) or C/EBPα expression vectors and cultured overnight in either high (25 mM) or low (5 mM) glucose medium. Cell lysates were immunoprecipitated with either rabbit anti-C/EBPα antibody or with rabbit IgG as control followed by immunoblotting. Immunoblots of immunoprecipitates (IP) and total lysates (Input) were stained as indicated.
(**H**) Immunoprecipitation (IP) of endogenous C/EBPα was performed with rabbit anti-C/EBPα antibody or with rabbit IgG as control from total lysates of Fao cells treated overnight with either DMSO or p300 inhibitor (C646, 10 μM). Immunoblots of immunoprecipitates (IP) and total lysates (Input) were stained as indicated.
(**I**) and (**J**) Immunoprecipitation (IP) of endogenous C/EBPα was performed with rabbit anti-C/EBPα antibody from total lysates of the liver tissues from mice fed either normal diet (ND), calorie restricted diet (CR) or high fat diet (HFD) as indicated. The immunoprecipitates (IP) and total lysates (Input) were analyzed by immunoblotting for C/EBPα, Acetylated K298-C/EBPα or β-actin loading control as indicated. For these experiments the C/EBPα-p30 isoform is shown while the IP levels of p42 isoform was too low (Figure S1F shows glucose dependent K298-acetylation of endogenous p42 and p30 in Fao cells as a control experiment). Bar chart at the right shows quantification of the relative changes in acetylated K298-C/EBPα/C/EBPα ratio upon different diets (n=4). Acetylated K298-C/EBPα/C/EBPα ratios were quantified by chemiluminescence and digital imaging. Statistical differences were analyzed by Student's t-tests. Error bars represent ±SD, *P<0.05, **P<0.01, ***P<0. 001. NS: not significant.

Lysine (K) 298 of C/EBPα was recently identified as an acetylation site using the anti-Ac-K298-C/EBPα antibody [21]. Using this antibody, a co-expression experiment with p300 in HEK293T cells showed that K298 of C/EBPα is also acetylated by p300 (**Figure S1E).** In addition, both the endogenously expressed C/EBPα isoforms p42 and p30 [22] in Fao cells are acetylated at K298, which is dependent on high glucose conditions (**Figure S1F).** Changes in nutrient and calorie intake can influence acetylation of regulatory proteins through changes in cellular concentrations of Acetyl-CoA and NAD+ [14,23]. To examine C/EBPα acetylation under different metabolic conditions *in vivo* we analyzed livers from mice that were either subject of calorie restriction (CR; 4 weeks) or high fat diet (HFD; 20 weeks). By using anti-Ac-K298-C/EBPα we found a decrease in C/EBPα K298-acetylation in livers of CR mice and an increase of its acetylation in livers of HFD mice (**Figure 1I and 1J;** shown is the p30-C/EBPα). Taken together, our data show that C/EBPα acetylation changes with nutritional status *in vivo*.

The immunoprecipitation experiments described above do not reveal to what extend or which of the lysines in C/EBPα are acetylated by p300 beyond K298. To

examine the distribution of lysine-acetylation, we purified acetylated C/EBPα protein derived from HEK293T cells co-expressing C/EBPα and p300 and examined protein acetylation by mass-spectrometric analysis (**Figure 2**). Of the fifteen lysines in C/EBPα, eleven were covered by the analyzed peptides of which five (K159, K250, K273, K275, K276) were found acetylated and six (K92, K169, K280, K304, K313, K352) not acetylated (**Figure 2**). Taken together, our analyses suggest that C/EBPα is subject of extensive acetylation mediated by p300 and that acetylation enhances its transactivation activity.

Peptide sequence	Mascot score	Position
PLVIKQEPR	59	K159
GPGGSLKGLAGPHPPDLR	54	K250
TGGGGGGGAGAGKAKKSVVDK	50	K273/K275/K276

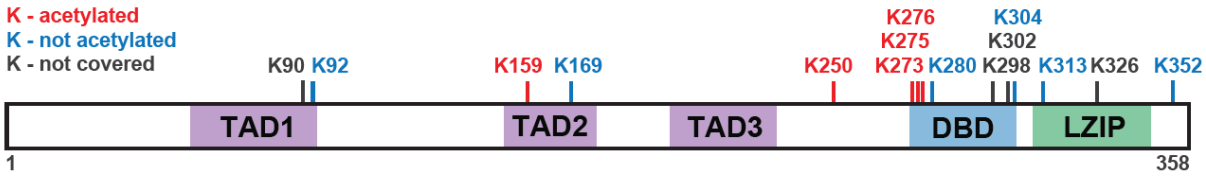

Figure 2. C/EBPα is acetylated by p300 at multiple lysines.
Mass spectrometry analyses identify the C/EBPα acetylation sites. HEK293T cells were transfected with expression plasmids for C/EBPα and p300-HA. C/EBPα protein was purified by immunoprecipitation using rabbit anti-C/EBPα antibody, digested with trypsin and analyzed by both MALDI-TOF and LC-ESI MS/MS. Mascot scores (upper panel) greater than 40 were most confident for the true detection of acetylation. The lower graph represents the C/EBPα protein with the acetylation status of its 15 lysines and locations of the transactivation domains (TAD), DNA-binding domain (DBD) and Leucine-zipper dimerization domain (LZIP).

C/EBPα binds to and is deacetylated by SIRT1

Lysine acetylation is a reversible PTM, which implies that specific lysine deacetylases (KDACs) may be responsible for C/EBPα deacetylation. The dependence of C/EBPα acetylation on glucose (**Figure 1A and 1G**) and the fact that C/EBPα and sirtuins both regulate glucose and fatty acid metabolism suggested that the NAD^+-dependent sirtuin deacetylases (SIRTs) could be involved. We examined the potential involvement of the four cytoplasmic and nuclear sirtuins, SIRT1, -2, -6 and -7 as well as SIRT3 that is mainly mitochondrial, however, may have nuclear functions in

addition [14]. The mitochondrial SIRT4 and SIRT5 that can act both in the mitochondria and cytosol [23,24] were not tested. To examine possible C/EBPα-sirtuin interactions C/EBPα was co-expressed together with one of the FLAG-tagged sirtuins in HEK293T cells. Co-immunoprecipitation using an anti-C/EBPα antibody followed by immunoblotting with an anti-FLAG antibody revealed that only SIRT1 interacts with C/EBPα (**Figure 3A**). The interaction between C/EBPα and SIRT1 was confirmed by reciprocal co-immunoprecipitation using an anti-FLAG antibody (**Figure 3B**). Next we examined the capacity of SIRT1 to deacetylate C/EBPα. HEK293T cells were co-transfected by C/EBPα and p300 expression plasmids to obtain acetylated C/EBPα in the presence of either SIRT1 or SIRT2 expression plasmids or empty vector control. Following C/EBPα immunoprecipitation, immunoblotting with an anti-HA or anti-Ac-K antibody showed binding to p300 and high level of C/EBPα acetylation, respectively, which are abrogated by co-expression of SIRT1 (**Figure 3C**). Co-expression of SIRT2, which does not interact with C/EBPα, has no effect on C/EBPα acetylation (**Figure 3C**). In addition, the ASEB computer algorithm (http://bioinfo.bjmu.edu.cn/huac/) [25] for prediction of SIRT1-mediated deacetylation lists all the mass-spectrometric identified lysines and K298 as potential SIRT1 deacetylation sites (**Table S1**). Furthermore, a progressive increase in expression levels of SIRT1 resulted in a progressive decrease in the acetylation level of C/EBPα (**Figure 3D**), which is accompanied by a progressive decrease in p300-dependent C/EBPα transactivation potential (**Figure 3E**). To examine whether C/EBPα-deacetylation by SIRT1 is attributed to the enzymatic activity of SIRT1 we set up an *in vitro* deacetylation assay. Purified FLAG-tagged acetylated C/EBPα was obtained by anti-FLAG-IP from HEK293T cells that were co-transfected with C/EBPα-FLAG and p300 expression plasmids. Purified FLAG-tagged SIRT1 was obtained separately by anti-FLAG-IP from HEK293T cells transfected with a SIRT1-FLAG expression plasmid. The deacetylation reaction assay revealed that SIRT1 efficiently deacetylates C/EBPα in the presence of NAD^+ *in vitro* (**Figure 3F**). Moreover, the deacetylation of C/EBPα by SIRT1 was inhibited in the presence of the sirtuin inhibitor nicotinamide (NAM). Taken together, our data show that lysine residues in C/EBPα can be deacetylated by SIRT1.

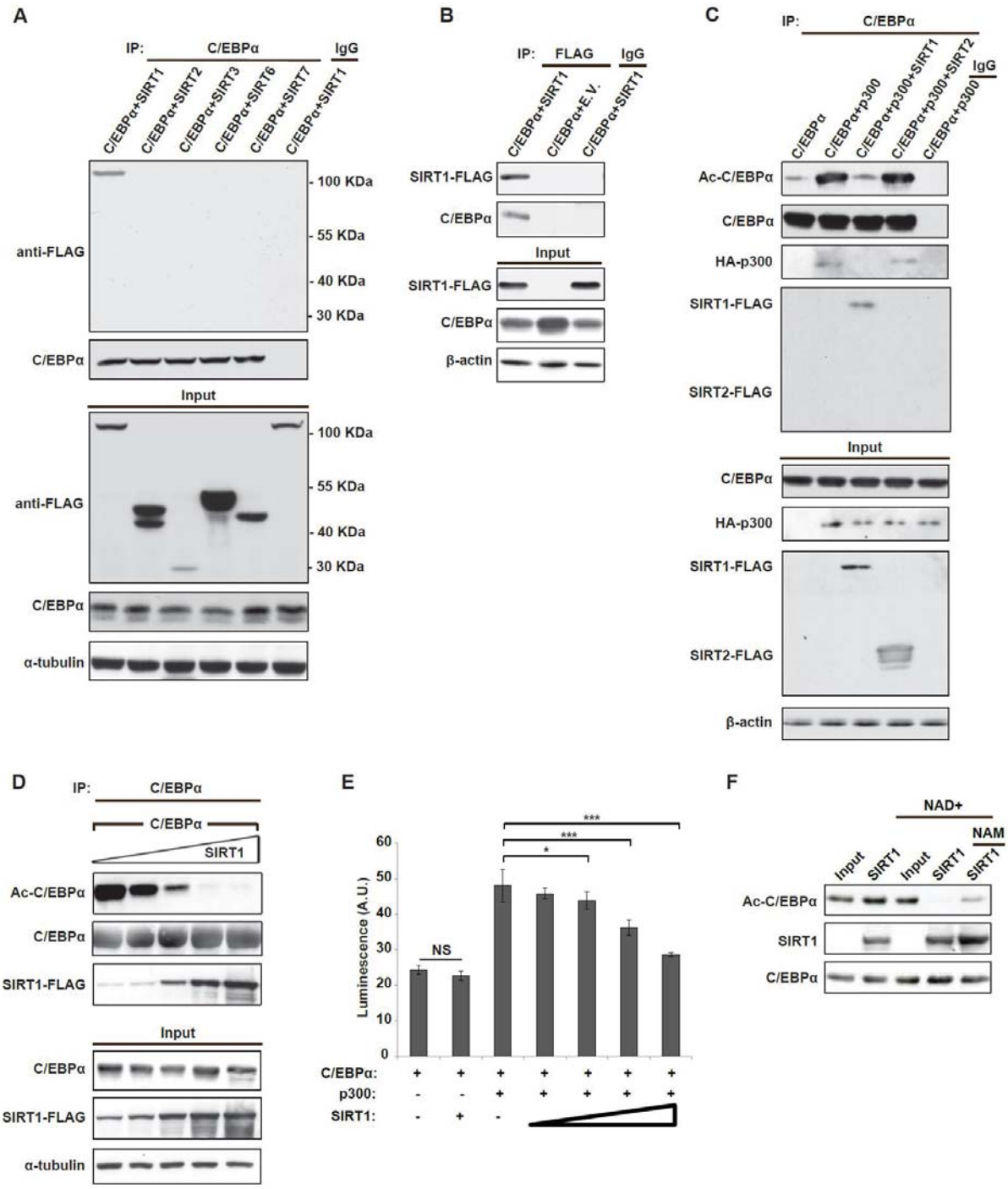

Figure 3. C/EBPα binds to and is deacetylated by SIRT1

(**A**) HEK293T cells were transfected with C/EBPα and one of the FLAG-tagged sirtuins expression vectors. Cell lysates were immunoprecipitated with rabbit anti-C/EBPα antibody or with rabbit IgG as control followed by immunoblotting. Immunoblots of immunoprecipitates (IP) and total lysates (Input) were stained as indicated.

(**B**) HEK293T cells were transfected with C/EBPα and either pcDNA3 empty vector (E.V.) or SIRT1-FLAG expression vectors. Cell lysates were immunoprecipitated with mouse anti-FLAG antibody or with mouse IgG as control followed by immunoblotting. Immunoblots of immunoprecipitates (IP) and total lysates (Input) were stained as indicated.

(**C**) HEK293T cells were transfected with C/EBPα, p300-HA, SIRT1-FLAG or SIRT2-FLAG expression vectors as indicated. Cell lysates were immunoprecipitated with rabbit anti-C/EBPα antibody or with rabbit IgG as control followed by immunoblotting. Immunoblots of immunoprecipitates (IP) and total lysates (Input) were stained as indicated.
(**D**) HEK293T cells were transfected with C/EBPα, p300-HA and increased amounts of SIRT1-FLAG expression vectors. Cell lysates were immunoprecipitated with rabbit anti-C/EBPα antibody or with rabbit IgG as control followed by immunoblotting. Immunoblots of immunoprecipitates (IP) and total lysates (Input) were stained as indicated.
(**E**) HEK293T cells were transiently transfected with luciferase C/EBPα responsive promoter vector, renilla expression vector for normalization, C/EBPα, p300-HA and increased amounts of SIRT1 expression vectors as indicated. Luciferase activity was measured 48 h later (n=3). Statistical differences were analyzed by Student's t-tests. Error bars represent ±SD, *P<0.05, **P<0.01, ***P<0.001. NS: not significant.
(**F**) In vitro SIRT1-deacetylation assay for C/EBPα. C/EBPα-FLAG and SIRT1-FLAG proteins were purified from HEK293 cells by immunoprecipitation with anti-FLAG M2 beads. The indicated proteins were incubated at 30 °C for 1 h with NAD+ or NAM where indicated, followed by immunoblotting with anti-acetylated lysine, anti-C/EBPα and anti-FLAG antibodies.

Acetylation of C/EBPα does not alter its subcellular localization or DNA-binding

Lysine acetylation of a transcription factor may serve to alter its transcriptional function, its DNA-binding properties or its subcellular localization [12]. We first examined whether the presence of either p300 or SIRT1 alters the subcellular localization of C/EBPα. Immunofluorescent staining of C/EBPα in HEK293T cells showed no difference in its nuclear localization between hyperacetylated C/EBPα derived from cells co-expressing p300 or hypoacetylated C/EBPα derived from cells co-expressing SIRT1 (**Figure 4A and S2A**). To determine whether co-expression of p300 or SIRT1 alters the binding of C/EBPα to a DNA recognition sequence purified (IP) FLAG-tagged C/EBPα wt was incubated with DNA oligonucleotide probes of either a C/EBP-consensus sequence or a mutated sequence and DNA-protein complexes were analyzed in an electrophoretic mobility shift analyses (EMSAs). SYBR Green DNA and SYPRO Ruby protein staining revealed that there is no difference in the DNA binding of C/EBPα between cells co-expressing p300 or co-expressing SIRT1 (**Figure 4B**). No DNA binding was detected with the C/EBPα-mutated binding sites. These data show that acetylation status of C/EBPα does not affect DNA binding in a significant way.

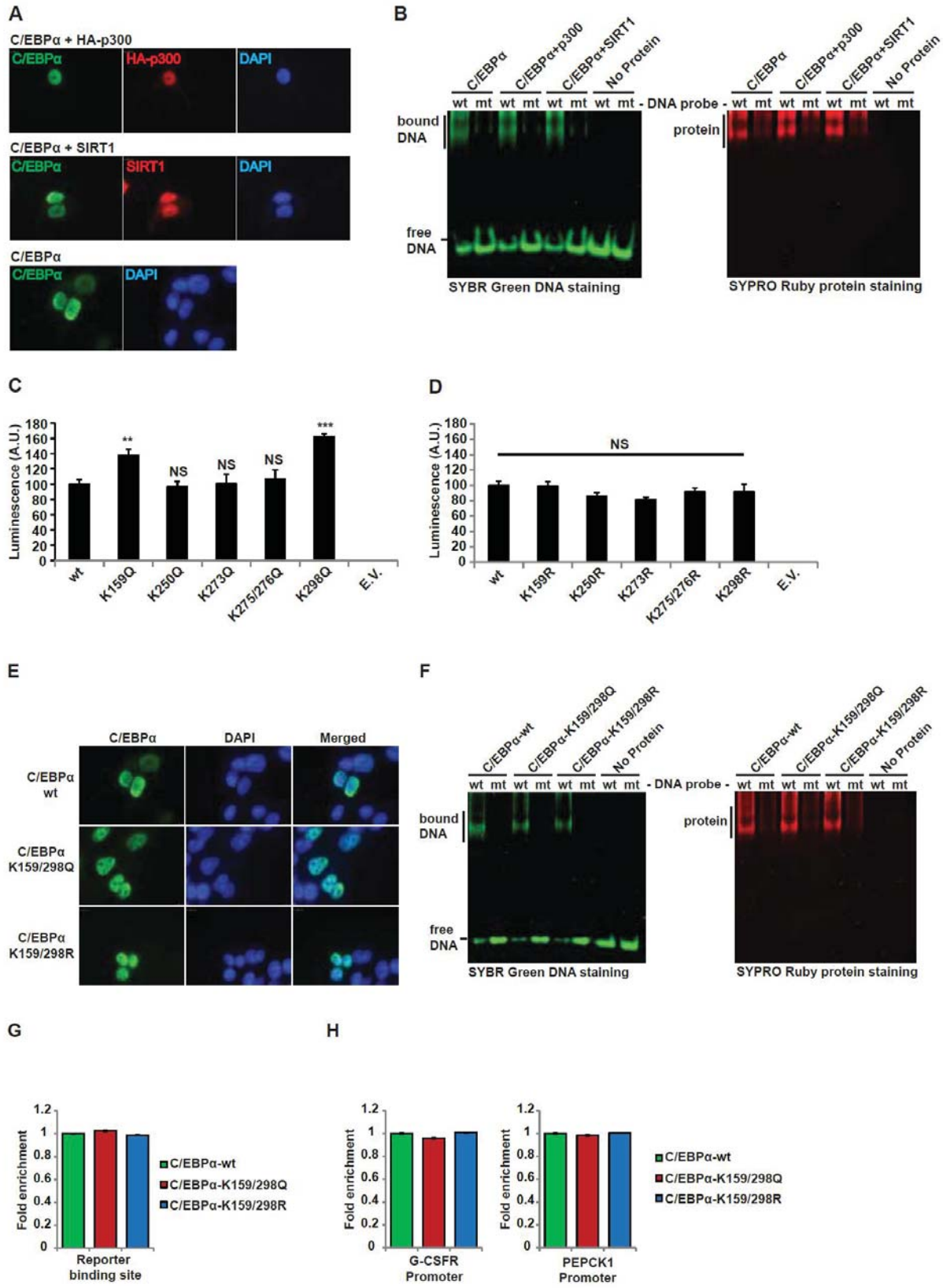

Figure 4. Acetylation of C/EBPα does not alter its subcellular localization or DNA-binding
(**A**) HEK293T cells were transiently transfected with C/EBPα alone, C/EBPα with p300-HA (acetylated) or C/EBPα with SIRT1-FLAG (deacetylated) expression vectors. Immunohistochemistry was

performed using anti-C/EBPα, anti-HA and anti-FLAG antibodies. DNA was stained with DAPI to visualize the nucleus. See Figure S2A for acetylation status of C/EBPα.
(**B**) HEK293T cells were transiently transfected with C/EBPα-FLAG alone, C/EBPα-FLAG with p300-HA (acetylated) or C/EBPα-FLAG with SIRT1 (non-acetylated) expression vectors. C/EBPα-FLAG protein was purified by immunoprecipitation with anti-FLAG M2 beads. EMSA was performed using a double-stranded oligonucleotides containing either wt or mutated (mt) C/EBPα binding site.
(**C**) and (**D**) HEK293T cells were transiently transfected with C/EBP-responsive luciferase reporter, renilla expression vector for normalization, wt C/EBPα or either (C) lysine to glutamine (KQ) or (D) lysine to arginine (KR) mutated C/EBPα expression vectors. Luciferase activity was measured 48 h later (n=3). Statistical differences were analyzed by Student's t-tests. Error bars represent ±SD, *P<0.05, **P<0.01, ***P<0. 001. NS: not significant.
(**E**) HEK293T cells were transiently transfected with wt, K159/298Q or K159/298R mutated C/EBPα-FLAG expression vectors. Immunohistochemistry was performed using anti-FLAG antibody. DNA was stained with DAPI to visualize the nucleus.
(**F**) HEK293T cells were transiently transfected with wt, K159/298Q or K159/298R mutated C/EBPα-FLAG expression vectors. C/EBPα proteins were purified by immunoprecipitation with anti-FLAG M2 beads. EMSA was performed using a double-stranded oligonucleotides containing either wt or mutated (mt) C/EBPα binding site.
(**G**) Fold enrichment of C/EBP binding site DNA used in the C/EBP-responsive firefly-reporter by DNA immunoprecipitation with wt-, K159/298Q- or K159/298R-C/EBPα-FLAG, using mouse anti-FLAG antibody versus non-specific mouse IgG. The experiment was performed in HEK293T cells, analyzed by quantitative real-time PCR. Mean ± s.d. (n=3).
(**H**) Fold enrichment of DNA from endogenous C/EBPα target genes G-CSFR and PEPCK1 obtained by chromatin immunoprecipitation (ChIP) with wt-, K159/298Q- or K159/298R-C/EBPα-FLAG, using mouse anti-FLAG antibody versus non-specific mouse IgG. The experiment was performed in HEK293T cells, analyzed by quantitative real-time PCR. Mean ± s.d. (n=3).

To examine the involvement of acetylation of individual C/EBPα lysines on the transactivation activity of C/EBPα we generated mutations that either mimic acetylation (Lysine (K) to Glutamine (Q)) or non-acetylation (Lysine (K) to Arginine (R)) at the acetylated lysines identified by mass spectrometry, K159, K250, K273, K275, K276 and the established acetylation site K298. **Figure 4C** shows that only the single K159Q or K298Q acetylation mimicking mutations in C/EBPα result in enhanced C/EBPα transactivation capacity compared to the wt C/EBPα, using the C/EBP-binding site reporter. None of the K-to-R acetylation preventing mutations altered the reporter activity (**Figure 4D**).

Next we examine subcellular localization of the dual K159Q/K298Q acetylation mimicking and K159R/K298R non-acetylation mutants of C/EBPα. Neither mutation affected the subcellular localization (**Figure 4E**). In addition, the mutations do not affect DNA binding in an EMSA (**Figure 4F**). Furthermore binding to the C/EBP-binding site in the reporter was not altered by the lysine mutations as was measured by C/EBPα-immunoprecipitation and qRT-PCR quantification of bound DNA

(**Figure 4G and S2B**). Finally, chromatin-immunoprecipitation (ChIP) experiments showed that there is no difference in binding between wt C/EBPα, the K159Q/K298Q C/EBPα mutant or K159R/K298R C/EBPα mutant to natural C/EBP binding sites in promoters of the endogenous genes G-CSFR and PEPCK1 (**Figures 4H and Figure S2B**). Therefore we conclude that acetylation of the lysines K159/K298 enhanced C/EBPα transactivation without affecting subcellular localization or DNA-binding.

Acetylation of Lysine 298 of C/EBPα stimulates acetylation of subsequent lysines

Next we asked whether prevention of acetylation of either K159, K298 or of all six lysines by K-to-R mutations affects p300-binding and acetylation or the transactivation potential of C/EBPα. K-to-R mutated C/EBPα mutants were co-expressed with p300 in HEK293T cells and p300-binding and C/EBPα-acetylation was analyzed after C/EBPα immunoprecipitation. Notably, the mutation K298R strongly reduced binding to p300 associated with a strong reduction in C/EBPα acetylation (**Figure 5A**). The K159R single mutation had no effect on p300-binding and C/EBPα-acetylation, although in the double mutant K159/298R the level of C/EBPα-acetylation is further decreased (**Figure 5A**). As expected, mutation of all six lysines (K159/250/273/275/276/298) in the K6R mutant reduces C/EBPα acetylation by p300 to very low levels. In accordance, the transactivation of the C/EBP-reporter is similar for co-expression of wt- or K159R-C/EBPα, decreased for K298R-C/EBPα and further decreased for K159/298R- and K6R-C/EBPα (**Figure 5B**). Complementary results were obtained with the opposite lysine-acetylation mimicking K-to-Q mutations. The K159Q mutant did not significantly improve binding of C/EBPα to p300 or C/EBPα-acetylation while with the K298Q mutant p300-binding and C/EBPα-acetylation is strongly increased, and there is a further increase for the double mutant K159/298Q (**Figure 5C**). The K6Q mutation also results in enhanced binding of p300 and a stronger acetylation signal although the anti-L-Ac antibody does not recognize the KQ mutations. This suggests that in the K6Q mutant, acetylation of other lysines increases that normally are not efficiently acetylated. Co-expression of the K-to-Q C/EBPα mutants, p300 and the luciferase C/EBP-reporter resulted in a gradual increase in reporter activity from K159Q- to K298Q- to K159/298Q- and K6Q- C/EBPα (**Figure 5D**). Finally, increasing amounts

of SIRT1 co-expression does not reduce the transactivation potential through deacetylation of either K159/298Q- or K6Q-C/EBPα (**Figure S3**). Together, these results suggest that K298-acetylation is a priming acetylation event stimulating the recruitment of p300, acetylation of K159 and further acetylation of C/EBPα.

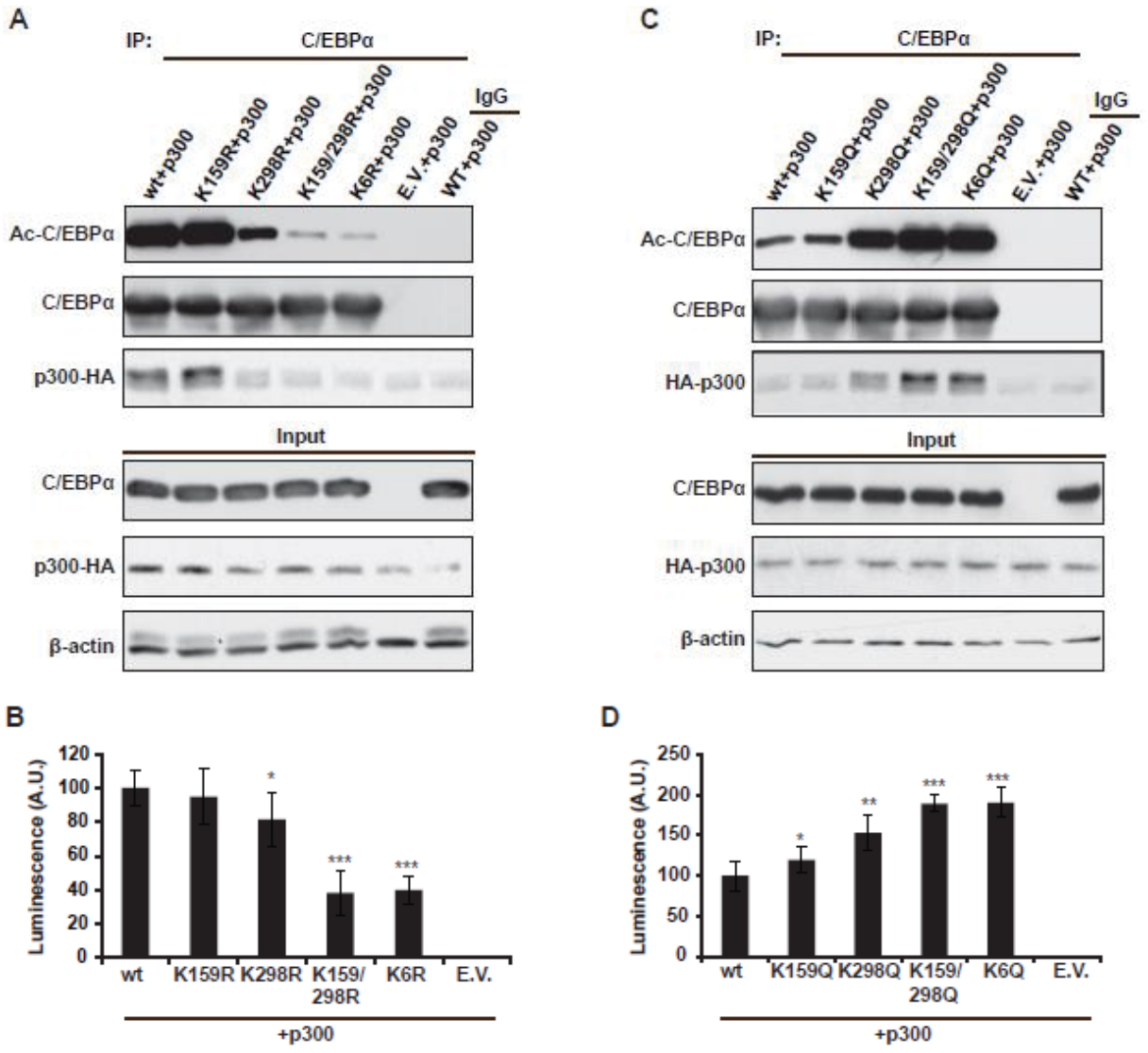

Figure 5. Acetylation of Lysine 298 of C/EBPα stimulates acetylation of subsequent lysines
(**A**) HEK293T cells were transiently transfected with p300-HA and either wt or one of the KR-C/EBPα mutant expression vectors. Cell lysates were immunoprecipitated with rabbit anti-C/EBPα antibody or with rabbit IgG as control followed by immunoblotting. Immunoblots of immunoprecipitates (IP) and total lysates (Input) were stained as indicated.
(**B**) HEK293T cells were transiently transfected with luciferase C/EBP-responsive firefly reporter, renilla expression vector for normalization, p300-HA and either wt or one of the KR-C/EBPα mutant expression vectors. Luciferase activity was measured 48 h later (n=3).
(**C**) HEK293T cells were transiently transfected with p300-HA and either wt or one of the KQ-C/EBPα mutant expression vectors. Cell lysates were immunoprecipitated with rabbit anti-C/EBPα antibody or

with rabbit IgG as control followed by immunoblotting. Immunoblots of immunoprecipitates (IP) and total lysates (Input) were stained as indicated.
(**D**) HEK293T cells were transiently transfected with luciferase C/EBP-responsive firefly reporter, renilla expression vector for normalization, p300-HA and either wt or one of the KR-C/EBPα mutant expression vectors. Luciferase activity was measured after 48 h (n=3).
Statistical differences were analyzed by Student's t-tests. Error bars represent ±SD, *P<0.05, **P<0.01, ***P<0. 001. NS: not significant. K6: K159/250/273/275/276/298.

C/EBPα acetylation status determines the C/EBPα-regulated transcriptome

To investigate the consequences of C/EBPα-acetylation on global C/EBPα-controlled gene transcription we generated Hepa1-6 mouse hepatoma cell lines with cumate-inducible expression of wt-, K159Q/K298Q- or K159R/K298R-C/EBPα-FLAG proteins (**Figure 6A**). Comparative transcriptome analysis identified 110 upregulated transcripts and 122 downregulated transcripts in the hypoacetylation K159R/K298R-C/EBPα mutant versus hyperacetylation K159Q/K298Q-C/EBPα mutant expressing cells (**Figure 6B**). We only considered genes to be differential regulated between the hypo- versus hyperacetylation C/EBPα mutants if their expression levels are intermediate in the wt C/EBPα expressing cells.

Ten of each up- or downregulation genes were re-analyzed by qRT-PCR confirming their regulation shown by the transcriptome analysis (**Figure 6C**). Gene ontology (GO) analysis using the DAVID database (Huang et al., 2009) revealed that the upregulated transcripts in the K159R/K298R-C/EBPα mutant expressing cells are enriched for genes in oxidation-reduction processes and mitochondrial biology, while the downregulated transcripts are enriched for glycoprotein genes (**Figure 6D and Table S2**). Most of the regulated genes have C/EBPβ-associated DNA fragments in the ENCODE database (http://genome.ucsc.edu/ENCODE/) (**Table S2**). C/EBPβ is closely related to C/EBPα and since they bind to the same recognition sequences C/EBPβ may substitute for C/EBPα for which data are not available. In the metabolic context these results suggest that deacetylation of C/EBPα is involved in the SIRT1 controlled increase in mitochondrial biogenesis and function under conditions of low glucose / low energy.

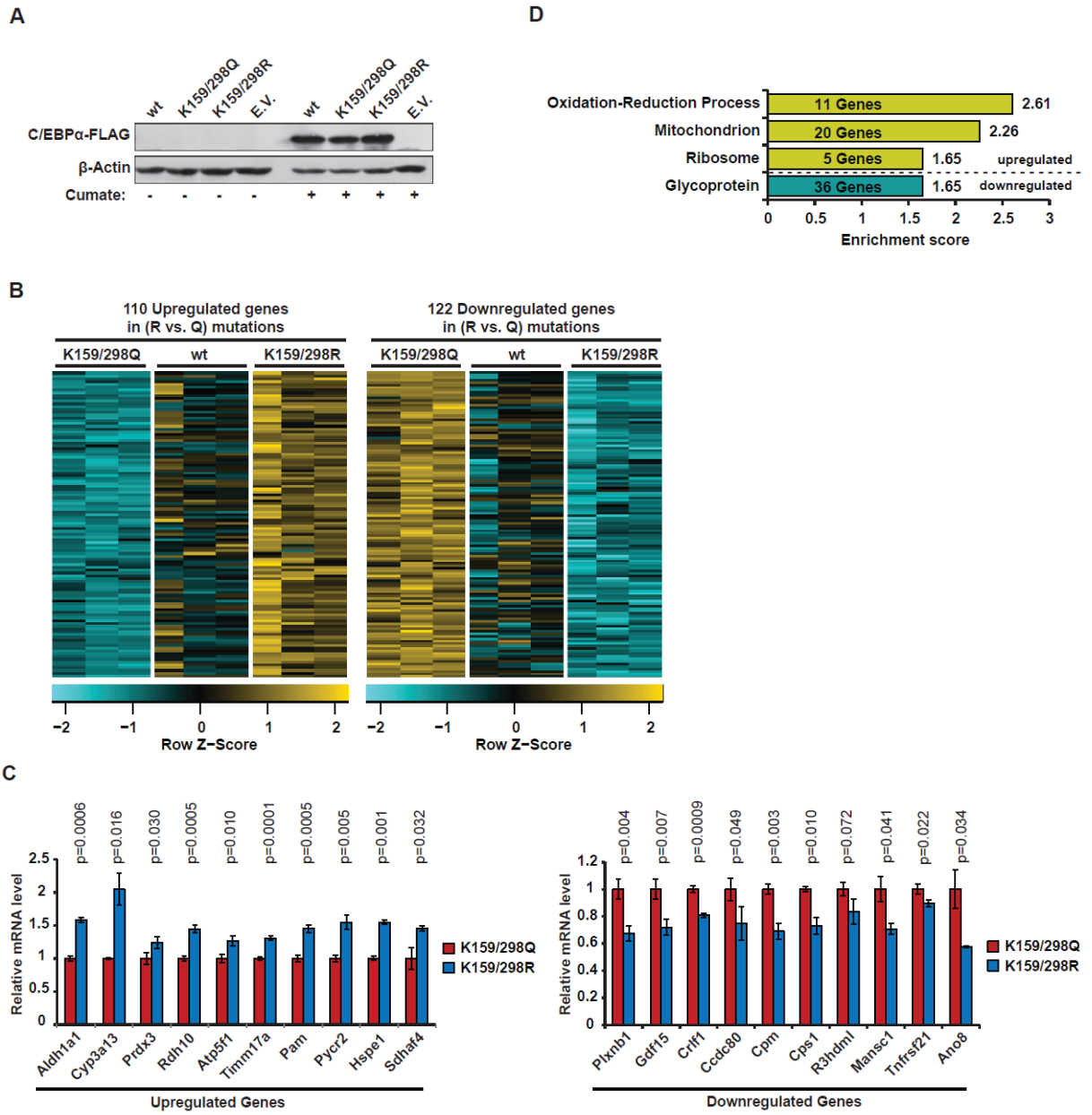

Figure 6. C/EBPα acetylation status determines the C/EBPα-regulated transcriptome

(**A**) Western blot analysis for Hepa1-6 cells stably transfected with empty vector (E.V.), wt-, K159/298Q-, K159/298R-C/EBPα-FLAG cumate-inducible constructs. Total lysates from Cumate-induced and non-induced cells were immunoblotted with anti-FLAG and anti-β-actin antibodies.

(**B**) Heat map of 232 differentially expressed genes (DEGs) in cumate-induced Hepa1-6 cells expressing K159/298R-C/EBPα-FLAG compared to the cells expressing K159/298Q-C/EBPα-FLAG as measured by RNA-seq. Low expression is shown in cyan, and high expression is in yellow. (FDR adjusted p value < 0.01 and the medians in the wt condition are located between the medians of K159/298Q and K159/298R). See Supplementary Table S2 for a complete list of DEGs.

(**C**) Relative mRNA expression levels (qRT-PCR) of 10 upregulated (left) and 10 downregulated (right) genes in cumate-induced Hepa1-6 cells expressing K159/298R-C/EBPα-FLAG compared to the cells expressing K159/298Q-C/EBPα-FLAG (n=3). Corresponding P-values are depicted as determined with Student's t-test. Error bars represent ±SD.

(**D**) Representative functional annotation clusters of upregulated and downregulated genes in the 232 DEGs (Davis analysis adjusted enrichment score > 1.3). See Supplementary Table S2 for the list of clustered genes.

Hypoacetylated C/EBPα enhances mitochondrial function

In line with a role of hypoacetylated C/EBPα in mitochondrial regulation we found that cumate-induction of the K159R/K298R-C/EBPα mutant in Hepa 1-6 cells that are cultured in acetylation-favoring high glucose medium results in increased accumulation of MitoTracker fluorescent dye as a measure for mitochondrial mass, compared to the hyperacetylation K159Q/K298Q- or wt-C/EBPα (**Figures 7A and S4A**). In addition, under low glucose deacetylation-favoring conditions (2.5 mM) wt reaches similar mitochondrial mass compared to hypoacetylation K159R/K298R-C/EBPα, while the acetylation mimicking K159Q/K298Q-C/EBPα fails to increase mitochondrial mass (**Figure 7A**). The relative mitochondrial DNA (mtDNA) copy number did not changes upon expression of the C/EBPα variants (**Figure S4B**). To examine whether C/EBPα is required for SIRT1-dependent induction of mitochondrial mass we stimulated SIRT1 activity by treatment with SIRT1 activator II and compared mitochondrial mass of cells with sh-C/EBPα knockdown to control sh-RNA. Treatment with SIRT1 activator II resulted in a clear increase in mitochondrial mass in control cells that was almost completely abrogated in C/EBPα knockdown cells (**Figure 7B**). Taken together these data show that deacetylation of C/EBPα is required for the SIRT1 induced increase in mitochondrial mass.

To investigate whether mitochondrial function is affected by the C/EBPα acetylation we measured using the Seahorse XF extracellular flux analyzer basal oxygen consumption rate (OCR), maximal OCR (treatment with mitochondrial uncoupler 2,4-dinitrophenol (DNP)) and spare respiratory capacity (SRC) as indicators of mitochondrial respiration. In addition, we measured extracellular acidification rate (ECAR) and maximal ECAR (treatment with oligomycin) as measurement of glycolysis. Under high glucose (25 mM) acetylation-favoring conditions, expression of the hypoacetylation K159/298R-C/EBPα mutant results in an increase in basal OCR, maximal OCR and SRC (**Figure 7C and S4C**). This indicates that the hypoacetylated C/EBPα induces mitochondrial respiration. In addition, the hypoacetylation K159/298R-C/EBPα mutant increases basal and maximal ECAR (**Figure 7D and S4D**).

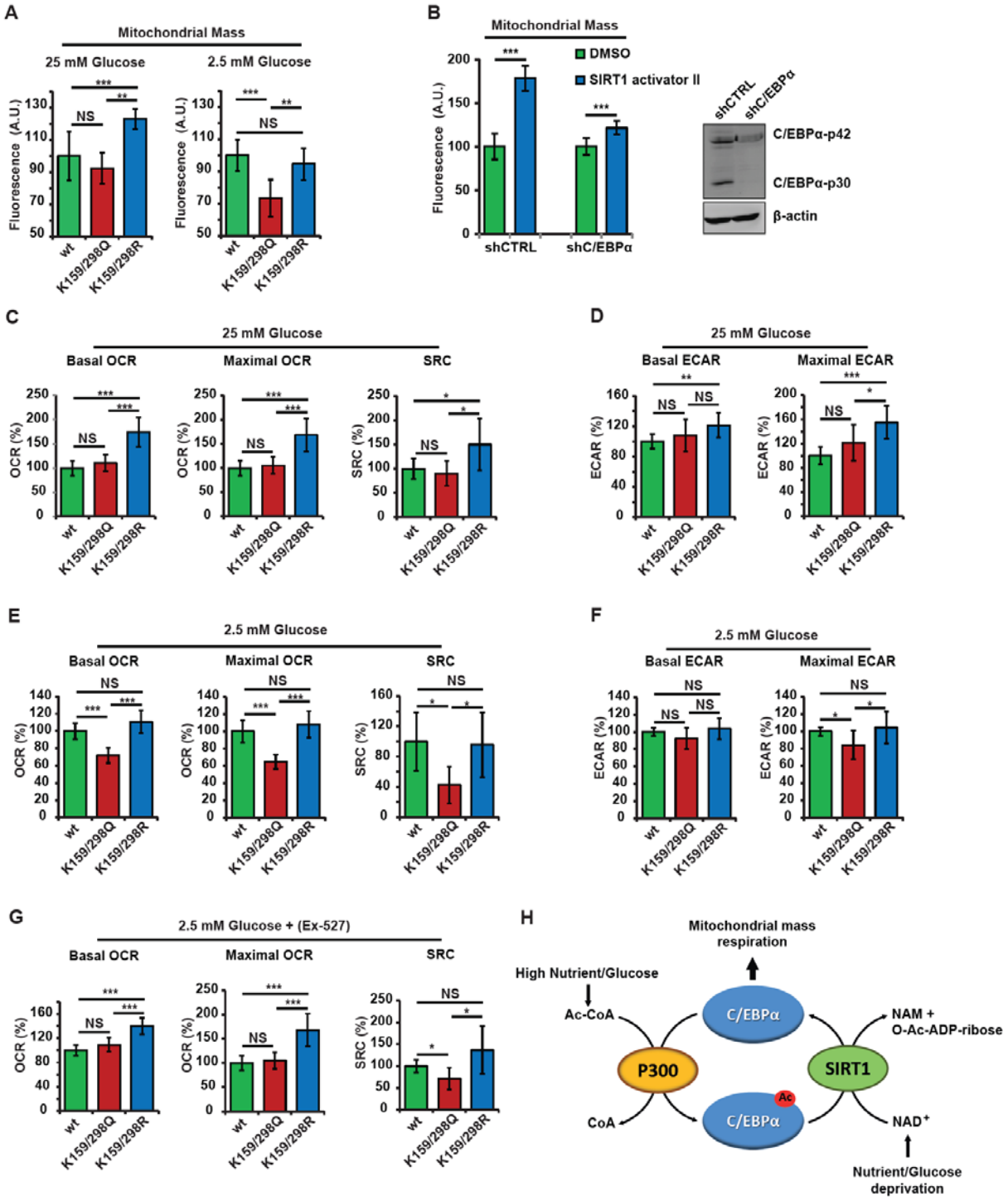

Figure 7. Hypoacetylated C/EBPα enhances mitochondrial function

(**A**) Cumate-induced Hepa1-6 cells expressing wt-, K159/298Q- or K159/298R-C/EBPα-FLAG were cultured in either high (25 mM) or low (2.5 mM) glucose medium then mitochondrial mass was measured with MitoTracker fluorescent dye.

(**B**) Hepa1-6 cells with C/EBPα knockdown (shC/EBPα) or control cells (shCTRL) were treated overnight with either DMSO as solvent or SIRT1 activator II. Mitochondrial mass was measured using MitoTracker fluorescent dye. Immunoblots of C/EBPα and β-actin loading control are shown at the far right.

(**C**), (**E**) and (**G**) Basal and maximal oxygen consumption rate (OCR) and spare respiratory capacity (SRC) in cumate-induced Hepa1-6 cells expressing wt-, K159/298Q- or K159/298R-C/EBPα-FLAG proteins and cultured in medium with 25 mM glucose (C), 2.5 mM glucose (E) or 2.5 mM glucose and treated with the SIRT1 inhibitor Ex-527 (Selisistat) 16 hours before the measurement (G).
(**D**) and (**F**) Basal and maximal extra cellular acidification rate (ECAR) in cumate-induced Hepa1-6 cells expressing wt-, K159/298Q- or K159/298R-C/EBPα-FLAG proteins and cultured in medium with 25 mM glucose (D) or 2.5 mM glucose (F).
For all experiments (n=5). Statistical differences were analyzed by Student's t-tests. Error bars represent ±SD, *P<0.05, **P<0.01, ***P<0. 001. NS: not significant.
(**H**) Model for a p300 and SIRT1 regulated acetylation switch of C/EBPα controlling mitochondrial function. P300 uses acetyl-CoA as substrate for the acetylation of C/EBPα under high nutrient/glucose conditions while under nutrient/glucose deprivation the high levels of NAD+ activate SIRT1 which deacetylates C/EBPα resulting in increased mitochondrial mass and respiration in the cell.

Under low glucose (2.5 mM) deacetylation-favoring conditions, expression of wt C/EBPα increased mitochondrial respiration (basal OCR, maximal OCR and SRC) to similar extends as the hypoacetylation K159/298R-C/EBPα mutant. Expression of the hyperacetylation K159/298Q-C/EBPα mutant did not result in a comparable increase in respiration (**Figure 7E and S4E**). Induction of the hypoacetylation K159/298R-C/EBPα did not increase ECAR compared to wt C/EBPα, while the K159/298Q-C/EBPα mutant mildly decreased the maximal ECAR (**Figure 7F and S4F**). These data indicate that induction of respiration by C/EBPα requires its lysine residues either to be available for deacetylation or being mutated to mimic hypoacetylation. To test whether SIRT1 activation is required for the induction of respiration by wt C/EBPα under low glucose conditions the cells were treated with the SIRT1 inhibitor Ex-527 (Selisistat), which completely inhibited the wt C/EBPα-induced basal OCR, maximal OCR and SRC under the low (2.5 mM) glucose deacetylation-favoring condition (**Figures 7G and S4G**).

Taken together, our data suggest that deacetylation of C/EBPα is part of the SIRT1-controlled increase in mitochondrial biogenesis and function (**Figure 7H**).

Discussion

In this study, we demonstrate that C/EBPα is acetylated by p300 and deacetylated by SIRT1 and that the acetylation status of C/EBPα determines its transcriptional functions. By using acetylation mimicking (KQ) or acetylation preventing (KR) mutations our data suggest that acetylation of lysine residue K298 primes for p300-

catalyzed acetylation at various additional lysines and that the K159/298Q dual mutation can substitute for maximal acetylation levels. We show that the acetylation status of C/EBPα modified either by p300, SIRT1, K159/298Q mutations or K159/298R mutations does not alter its cellular localization or DNA binding. Whole coding transcriptome analysis revealed that the hypoacetylation K159/298R-C/EBPα mutant induces transcripts involved in mitochondrial function and oxidation-reduction processes. Accordingly, expression of K159/298R-C/EBPα increases mitochondrial mass and respiration whereas C/EBPα knockdown abrogates the increase in mitochondrial mass induced by SIRT1 activation. Furthermore, inhibition of SIRT1 blunts wt C/EBPα-induced mitochondrial respiration under low glucose conditions. Our data fit into a model where C/EBPα functions downstream of SIRT1 to transcriptionally adapt mitochondrial function in response to alterations in the cellular energy/nutrition state (**Figure 7H**). The more subtle increase in ECAR upon K159/298R-C/EBPα induction, suggesting an increase in glycolysis, is only observed under high glucose conditions. Possibly, the higher metabolic (respiration) rate of the K159/298R-C/EBPα expressing cells allows for more glucose uptake under high glucose conditions that is constrained by low glucose availability.

The C/EBPα acetylation switch involving p300 and SIRT1 is reminiscent to the acetylation of C/EBPε regulated by these same factors [26]. C/EBPε is exclusively expressed in myeloid cells and acetylation of two lysines (K121 and K198) is indispensable for C/EBPε induced terminal neutrophil differentiation. C/EBPε-K121 is homologues to K159 of C/EBPα and both are subject of sumoylation and C/EBPε-K198 is homologues to K276 that we found acetylated in C/EBPα, further supporting the similarities in the acetylation of both proteins. In compliance with our results p300-mediated acetylation of C/EBPε enhances transactivation of a C/EBP-binding site containing M-CSFR-promoter reporter and the acetylation status does not affects cellular localization of C/EBPε. In contrast to our findings obtained with deacetylated C/EBPα, non-acetylated C/EBPε mutations are shown to reduce DNA binding, however, DNA-binding of wt C/EBPε upon co-transfection with p300 or SIRT1 was not investigated [26].

It has been shown earlier that C/EBPα expression is essential for mitochondrial biogenesis and proper expression of both nuclear and mitochondrial-genome encoded genes in brown fat [27]. Our report is the first to show that this

function of C/EBPα depends on the hypoacetylated state of C/EBPα that is provided by the energy sensing deacetylase SIRT1, suggesting that C/EBPα mediates effects of SIRT1 on mitochondrial function. This is corroborated by the finding that the reduction of glucose concentration can induce mitochondrial respiration in wt C/EBPα expressing cells but not in cells expressing either the acetylation mimicking K159/298Q-C/EBPα mutant or the hypoacetylated K159/298R-C/EBPα mutant; while K159/298R mutant has already increased mitochondrial respiration at high glucose concentrations compared to wt C/EBPα the respiration stays at a low level in the K159/298Q mutant expressing cells.

SIRT1 is known to control mitochondrial biogenesis and gene expression by deacetylating the transcriptional coactivator peroxisome proliferator-activated receptor gamma coactivator 1-alpha (PGC1α) [14,28-30]. In addition, SIRT1 controls the acetylation and function of forkhead box O (FOXO) transcription factors, which are important regulators of lipid and glucose metabolism as well as of stress responses [14,31-33]. SIRT1 regulates adiponectin gene expression through stimulation of a FOXO1-C/EBPα transcriptional complex [34]. Here, FOXO1 is thought to be the target and deacetylated by SIRT1, however, deacetylation of C/EBPα was not investigated in this study. By using a hypoacetylation (K159/298R) mutant we demonstrate that C/EBPα deacetylation alone is sufficient for stimulating mitochondrial function. Whether deacetylated C/EBPα induces PGC1α expression (eventually in collaboration with FOXO transcription factors), collaborates with PGC1α in the activation of mitochondrial genes or whether it acts independently from PCG1α has to be analyzed in future experiments.

Recently, Bararia et al showed that C/EBPα is acetylated by the KAT GCN5 at lysines K298, K302 in the DNA binding domain and K326 in the leucine zipper dimerization domain by using *in vitro* acetylation of short C/EBPα peptides and confirmation by mass-spectrometry and western blotting using specific antibodies raised against acetylated C/EBPα [22]. In the latter study, acetylated C/EBPα was found enriched in human myeloid leukemia cell lines and primary acute myeloid leukemia (AML) samples, and the data show that C/EBPα acetylation results in impaired DNA binding and thus loss of transcriptional activity resulting in inhibition of C/EBPα granulopoietic function. We did not observe effects on DNA binding per se between hypo- or hyperacetylated C/EBPα. These differences may be the result of the different

mutations used and the different experimental systems, hematopoietic cells in the Bararia et al study versus HEK293T and liver Hepa 1-6 cells in our study. Bararia et al show loss of DNA-binding and transactivation activity using dual K298Q/K302Q or triple K298Q/K302Q/K326Q mutants that all reside in the bZIP DNA-binding domain [22]. Importantly, they report that single acetylation mimetics of one of the three lysines show no effect on DNA binding and transactivation. In our mass spectrometry analysis K298Q, K302Q and K326Q were not covered. K298 is predicted to be acetylated by p300 and deacetylated by SIRT1 (**Table S1**) and was identified as p300 acetylation site by using Ac-K298 specific antibodies [22]. We did not include K302 and K326 since these are not predicted as targets for p300 or SIRT1 (**Table S1**). Here we examined the dual K159Q/K298Q mutation of which K159 lies outside the bZIP domain. Since we also do not see any effect on DNA binding with co-transfection of p300 and rather a stimulation of reporter promoter activity, we believe that at least in the experimental systems we use acetylation of C/EBPα does not alter DNA-binding. Bararia et al [22] found that co-transfection of p300 and C/EBPα results in stimulation of a C/EBP-binding site reporter, while co-transfection with GCN5 represses the reporter. Similar to these results and to other studies we also found that co-expression of p300 and C/EBPα stimulates a C/EBP-dependent promoter reporter [16,22], however, in our system GCN5 did not alter the reporter activation in a dose dependent manner (although GCN5 binds C/EBPα). Possibly, in different cellular systems acetylation of C/EBPα can occur at different lysine residues by different KATs with different outcomes on DNA binding and / or transactivation. Different KAT regulatory pathways, C/EBPα interacting proteins or other posttranslational modifications of C/EBPα might influence this process. Overall, our data are more in agreement with the effects of acetylation and deacetylation of C/EBPε by p300 and SIRT1 [26], as was discussed above.

C/EBPα is subject of extensive PTMs, including phosphorylation, methylation, sumoylation and ubiquitination [35,36]. Sumoylation of C/EBPα at lysine residue K159 reduces C/EBPα-transactivation of the albumin gene in fetal primary hepatocytes and abrogates the interaction with Brahma-Related Gene-1 (BRG1) resulting in reduced inhibitory effect on cell proliferation [37,38]. Acetylation and sumoylation at K159 are obviously mutually exclusive and prevention of sumoylation by acetylation could be involved in the observed higher transcriptional efficacy of the K159Q mutant

measured with the C/EBP-binding site reporter. However, the K159R that similarly prevents sumoylation at this site shows no enhanced activity, suggesting that lysine-acetylation modulates the transcriptional activity of C/EBPα through other mechanisms.

Our luciferase reporter studies using KQ mutants suggest that acetylation of C/EBPα increases its transcriptional functions. However, we do not know whether the involved KATs (p300 in case of C/EBPα) stimulate the transcriptional activity through acetylation of C/EBPα itself or also through acetylation of other involved transcriptional (co)factors. Since acetylated C/EBPα and the hyperacetylation K159/298Q mutant seem to have a higher binding affinity to p300 the higher reporter activity observed could be explained by a stronger recruitment of p300 through acetylated C/EBPα. The hypoacetylated K159R or K298R C/EBPα mutants do not modulate the transcription from the C/EBP-dependent promoter reporter in the absence of p300 (**Figure 3D**), however, downregulates the reporter in the presence of p300, which goes along with reduced p300-C/EBPα interaction. The lack of transcriptional stimulation of the K159/298R-C/EBPα mutant may seem at odds with the observed upregulation of genes in the transcriptome analysis by this mutant. So far we do not know whether the observed changes in the transcriptome are a result of direct promoter regulation through C/EBPα or an indirect effect. Thus, the acetylation state of C/EBPα might discriminate between interaction partners and/or co-factors (e.g. p300) and thereby affect different promoters in opposite ways. Such sophisticated regulatory mechanisms are difficult to measure using a simple reporter construct containing only C/EBP binding sites. The finding of upregulated genes in cells expressing the hyperacetylation K159/298Q-C/EBPα mutant that fall into different GO-term categories compared to those induced by the hypoacetylation K159/298R-C/EBPα mutant speaks in favor of such a scenario.

Taken together our results suggest that C/EBPα acetylation depends on nutrient (glucose) availability and is negatively controlled by the class III lysine deacetylase SIRT1. Our observations that hypoacetylation mimicking C/EBPα mutant expressing cells show increased expression of mitochondrial genes, higher mitochondrial mass and mitochondrial respiration propose C/EBPα as critical downstream mediator of SIRT1 mitochondrial function.

Materials and Methods

DNA constructs. The pcDNA3-based rat C/EBPα and rat C/EBPα-FLAG have been described earlier [39]. Mutations were introduced by either site-directed mutagenesis or exchange of wt sequences by mutated DNA-fragment oligonucleotides by cloning. Cloning details are available upon request. Cumate-inducible constructs were obtained by cloning rat C/EBPα sequences from pCDNA3-based K159/298Q-FLAG, K159/298R-FLAG and wt C/EBPα-FLAG into SparQ All-in-one Cumate Switch Vector (#QM812B-1, System Bioscience Inc). p300-HA, ΔKAT-p300-HA expression vectors were described in [40], P/CAF-FLAG in [41] and Tip60 in [42]. SIRT1-FLAG, SIRT2-FLAG, SIRT3-FLAG, SIRT6-FLAG, SIRT7-FLAG, CBP-FLAG and GCN5-FLAG were obtained from Addgene (plasmid #13812, #13813, #13814, #13817, #13818, #32908 and #74784 respectively).

Cell culture, transfection and immunofluorescence. All cells were cultured in DMEM plus 10% FCS (Invitrogen) and penicillin/streptomycin at 5% CO_2 and 37° C. HEK293T cells were seeded at 2.5×10^6 cell in 10 cm dishes and transfected the next day with 5 µg expression vectors using calcium phosphate. Immunofluorescence staining protocol was described previously [39]. The primary antibodies used were anti-C/EBPα (14AA, Santa Cruz Biotechnology), anti-FLAG (M2, #F3165, Sigma) and anti-HA (#MMS-101R, Convace). Secondary antibodies used were Alexa Fluor 488 or 568 conjugated (Invitrogen). p300 inhibitor C646 (CAS 328968-36-1; Sigma-Aldrich) was used at final concentration of 10 µM.

Co-immunoprecipitation. Co-immunoprecipitation was performed as described previously by [39]. Anti-C/EBPα (14AA, Santacruz), anti-FLAG (M2, #F3165, Sigma), anti-HA (#MMS-101R, Convace) and anti-Tip60 (#NBP2-20647, Novus Biologicals) were used for precipitation as indicated. To detect the acetylation of C/EBPα in Fao cells, endogenous level, or in transiently transfected HEK293T cells, the cells were treated with the deacetylase inhibitors 1 µM TSA (#T8552, Sigma) and 5 mM nicotinamide (#47865U, Sigma) 8 h before harvesting. The IP lysis buffer and IP wash buffer were supplemented with these inhibitors as well.

Western blotting. Western blotting was performed following a general protocol. The following antibodies were used: anti-C/EBPα (14AA), anti-SIRT1 (H-300), anti-α-tubulin (TU-02), anti-p300 (C-20) and anti-P/CAF (H-369) (Santa Cruz Biotechnology); anti-acetyl-Lys (# 05-515, clone 4G12, Millipore); anti-FLAG (M2, #F3165, Sigma); anti-HA (#MMS-101R, Convace); anti-β-actin (clone C4, #691001,MP Biomedicals). and Anti-Tip60 (#NBP2-20647, Novus Biologicals) and anti-Ac-K298-C/EBPα [22]. HRP-conjugated secondary antibodies were purchased from Amersham Life Technologies. The bands were visualized by chemiluminescence (ECL, Amersham Life Technologies).

Luciferase assay. The luciferase construct containing two consensus C/EBPα binding sites site (pM82; lacking the AP-1 binding site) was described earlier [20]. For the Luciferase assay, 25000 HEK293T cells per well were seeded in 96-well plates. After 24 h, cells were cotransfected with the Luciferase reporter, Renilla expression vector and other expression vectors as indicated using FuGENE HD (Promega). After 48 h, Luciferase activity was measured by Dual-Glo Luciferase Assay System (#2920, Promega) following the manufacturer's protocol using a GloMax-Multi Detection System (Promega).

In vitro de-acetylation. *In vitro* deacetylation assay was performed as described by [43]. Acetylated C/EBPα was obtained by co-transfecting HEK293T cells with C/EBPα-FLAG and p300 expression plasmids. Cells were treated with 10 μM TSA and 5 mM nicotinamide 8 h before harvest. Anti-FLAG M2 beads (#M8823, Sigma) were used for precipitation and 3X-FLAG peptide (F4799, Sigma) was used for elution.

Lentiviral transduction and Cumate inducible system. Hepa1-6 cells were infected with SparQ All-in-one Cumate Switch Vector (#QM812B-1, System Bioscience Inc) containing either wt rC/EBPα-FLAG cDNA, K159/298Q-rC/EBPα-FLAG cDNA, K159/298R-rC/EBPα-FLAG cDNA or empty vector and propagated under puromycin selection (1.5 mg/ml). Cumate-inducing solution was added to the cells at a dilution (1:1000) 3 days before any experiment. To obtain the C/EBPα-KD

Hepa1-6 cells, the cells were infected with pLKO.1 lentiviral constructs containing shRNAs against mouse C/EBPα: sh:5'- CCG GCA ACG CAA CGT GGA GAC GCA ACT CGA GTT GCG TCT CCA CGT TGC GTT GTT TTT-3' or non-target shRNA control (Sigma-Aldrich) and propagated under puromycin selection (1.5 mg/ml).

Electrophoretic Mobility Shift Assay (EMSA). HEK293T cells were transfected with expression vectors by the calcium phosphate method. Anti-FLAG M2 beads (#M8823, Sigma) were used for precipitating C/EBPα-FLAG and 3X-FLAG peptide (F4799, Sigma) was used for elution. Purified C/EBPα-FLAG was incubated with double strand oligodeoxynuclotides containing either C/EBP consensus binding site or mutated one. The sense and antisense sequences are as follows: C/EBP consensus; sense 5′ CTA GCA TCT GCA G**AT** TGC GCA AT**C** TGC AC 3′; antisense 5′ TCG AGT GCA G**AT** TGC GCA AT**C** TGC AGA TG 3′. Mutant C/EBP consensus; sense 5′ CTA GCA TCT GCA G**AG** GTA TAC C**T**C TGC AC 3′; antisense 5′ TCG AGT GCA G**AG** GTA TAC C**T**C TGC AGA TG 3′. The C/EBP consensus and mutant sequences are underlined. C/EBPα DNA binding affinity was analyzed using Electrophoretic Mobility Shift Assay (EMSA) Kit, with SYBR® Green & SYPRO® Ruby EMSA stain (#E33075, Thermo Fisher Scientific) following the manufacturer's protocol.

Measurement of oxygen consumption rate (OCR). Oxygen consumption rates (OCR) and extracellular acidification rates (ECAR) were determined using a Seahorse XF96 Extracellular Flux analyzer (Seahorse Bioscience). 2.5×10^4 of cumate-induced Hepa1–6 cells per well were seeded into a 96-well XF cell culture microplate 24 h prior to the assay. Sixteen hours before the assay, the culture medium was changed to new medium with the indicated glucose concentration supplied with cumate solution. One hour before the assay, the cells were washed twice and incubated with pre-warmed Seahorse assay media supplemented with the same concentration of glucose that the cells were having. Maximal OCR was measured after DNP (2,4-Dinitrophenol) injection at final concentration of 50 μM. Spare respiratory capacity (SRC) was calculated as the difference between basal and maximal OCR. Maximal ECAR was measured after oligomycin injection at final concentration of 2.5 μM. The SIRT1 inhibitor Ex-527 (Selisistat) (CAS 49843-98-3; Sigma-Aldrich) was used at final concentration of 10 μM.

Mass Spectrometry analysis. HEK293T cells were transiently transfected with C/EBPα and p300-HA expression vectors. C/EBPα was immunoprecipitated using rabbit anti-C/EBPα antibody followed SDS-PAGE and the proper C/EBPα protein band cut and used for further MS protocol. The bands were washed with water and destained by 3 rounds of incubation in 70 % acetonitrile (ACN) followed by incubation in 25 mM ammonium bicarbonate in water (AmBic). The gel pieces were reduced with 10 mM dithiothreitol in AmBiC for 20 min und alkylated with 50 mM iodoacetamide in AmBic for 20 min. After washing with 3 changes of AmBic followed by 70 % ACN the gels were dried. The samples were in-gel digested using one of the following proteases: trypsin (Serva), chymotrypsin (Roche), or Arg-C (Roche). To this aim the tubes containing the dried gel pieces were placed in an ice-water bath and the gels covered with solutions of the proteases (5 ng/µl for trypsin, 25 ng/µl for other proteases) in digestion buffer (8 %ACN, 25 mM ammonium bicarbonate, 1 mM calcium chloride in water). After 40 min incubation in the ice-water bath the supernatants were completely removed and the gel pieces covered with digestion buffer. Digestion was performed overnight at 37 °C. The supernatants were transferred to fresh vials and the gels extracted with 0.1 % trifluoroacetic acid, 33 % ACN in water for 15 min. The supernatants were combined with those from the digestion and a second extraction of the gel pieces was performed with 70 % ACN in water. The supernatants were combined with those from the former steps and the samples were evaporated in a SpeedVac (Christ) to dryness. For analysis by LC-MS/MS the samples were dissolved in 25 µl HPLC buffer A (5 % ACN, 0.1 % formic acid in water). An aliquot of 5 µl was applied for nano LC separation by an eksigent 2D nanoLC system (eksigent, Dublin, USA) using a trap column (20 mm x 0.1 mm, nanoseparations, Netherlands) and a separation column (150 mm x 0.075 mm, nanoseparations, Netherlands). Elution of the bound compounds was performed at a flow of 300 nl/min with a linear gradient of 0 to 36 % HPLC buffer B (80 %ACN, 0.1% formic acid) versus HPLC buffer A within 60 minutes. The eluent was directly sprayed into the orifice of an LTQ Orbitrap XL ETD (ThermoScientific, Dreieich, Germany) mass spectrometer. The data acquisition by the mass spectrometer was controlled by the Xcalibur software(ThermoScientific, Dreieich, Germany) and a top 3 approach was selected. This consisted of cycles of recording a survey spectrum at 60000 resolution and successively selecting the 3 most abundant entities with a

charge state equal to or higher than 2 for fragmentation by CID in the linear ion trap. The spectra were processed and analyzed with the software package ProteomeDiscoverer 1.4 (ThermoScientific, Dreieich, Germany) using Mascot 2.1 as the search engine and SwissProt as the protein data base. Carbamidomethylation of Cys was set as fixed modification and oxidation of Met and acetylation of Lys were allowed as variable modifications. To enhance the chance of identification of acetylated peptides containing internal lysine residues the number of allowed miss cleavages was set to 2 or 3. The coverages of C/EBPα proteins by detected peptides were in the range between 5 % and 40 % depending on the used IP sample and the protease used for digestion. The best results were obtained with trypsin digestion which enabled the identification of the highest number of acetylation sites with high Mascot scores.

RNA-seq Analysis. Transcriptome analysis was done in triplicates. Hepa1-6 cells treated for three days with cumate solution to express wt-, K159/298Q- and K159/298R- C/EBPα proteins were harvested and the total RNAs were isolated using RNeasy Plus mini Kit (#74136, Qiagen) according to the manufacturer's protocol. Sequencing libraries were prepared using the TruSeq Sample Preparation V2 Kit (#RS-122-2002) according to manufacturer's instructions. cDNA libraries were subjected to high-throughput single-end sequencing (65 bp) in an Illumina HiSeq 2500 instrument. Reads were aligned and quantified using STAR 2.5.2a (Dobin et al, 2013, PMID: 23104886), against primary assembly GRCh38 using Ensembl gene build 84 (http://www.ensembl.org). Genes with average expression level below 1 fragment per million (FPM) were excluded from the analysis. A generalized linear model was used to identify differential gene expression using EdgeR package [44,45]. Only those genes are shown of which the medians in the wt condition are located between the medians of K159/298Q and K159/298R. The library normalization was left at the standard setting (trimmed mean of M-values, TMM). The resulting p-values were corrected for multiple testing using the Benjamini-Hochberg procedure. Data visualization and statistical tests were conducted using custom R scripts (available upon request). Gene ontology (GO) analysis was performed using the DAVID database version 6.8 [46] with default DAVID database setting with medium stringency and Mus musculus background. C/EBPβ-associated DNA fragments for

the regulated genes (Table S2) were detected using the ENCODE database (http://genome.ucsc.edu/ENCODE/) in sequences up to 10 Kb upstream of the transcription start sites.

Quantitative Real-Time PCR analysis. Total RNA was isolated using the RNeasy Kit (QIAGEN). For cDNA synthesis 1µg RNA was reverse transcribed with the Transcriptor First Strand cDNA Synthesis Kit (Roche) using Oligo(d)T primers. qRT-PCR was performed using the LightCycler® 480 SYBR Green I Master Mix (Roche). The following primer pairs were used for β-actin for normalization: 5′-aga ggg aaa tcg tgc gtg ac-3′ and 5′-caa tag tga tga cct ggc cgt-3′. The other used primer pairs are listed in **Table S3**.

Chromatin and reporter C/EBP-binding site immunoprecipitation. HEK293T cells were transfected with wt-, K159/298Q- or K159/298R-C/EBPα expression vectors for the chromatin IP. HEK293T cells were cotransfected with C/EBP-binding site reporter construct and wt-, K159/298Q- or K159/298R-C/EBPα-FLAG expression vectors for the C/EBP-binding site IP. ChIP assay was performed with 5×10^6 cells using a Bioruptor (Diagenode, Inc.) for sonication (details on request). ChIP antibodies were against FLAG (M2, #F3165, Sigma) and non-specific mouse IgG from Santa Cruz Biotechnology. The fold enrichment was calculated relative to the background detected with non-specific rabbit IgG. For the semi-quantitative PCR, 1/50 (1 µl) of DNA obtained from the ChIP assay was used as template in a PCR reaction with 28 cycles. Primer pairs were for C/EBPα reporter (117 bp) 5′ GTC CAA ACT CAT CAA TGT ATC 3′ and 5′ CGA TCG GGG CAT TTT ATA G 3′, for G-CSFR Promoter (218 bp) 5′ ATT CCC CAG CCC TTT AAG AC 3′ and 5′ CTG CAG TCC AGC TTC TCT CC 3′ for PEPCK1 Promoter (331 bp) 5′ GAC TGT GAC CTT TGA CTA TGG GGT GAC ATC 3′ and 5′ CTG GAT CAC GGC CAG GGT CAG TTA TGC 3′.

Mitochondrial content and mtDNA copy mumber. Mitochondrial mass was measured using MitoTracker Red 480 kit following the manufacturer's protocol (#M22425, ThermoFisher). Fluorescence was measured using a GloMax-Multi Detection System (Promega). SIRT1 Activator II (CAS 374922-43-7; Merck #566313)

was used at final concentration of 10 μM. Mitochondrial DNA was co-purified with genomic DNA from Hepa1-6 cells using standard protocol, Ct values determined for cytochrome b gene encoded by mtDNA and β-actin gene encoded by the nuclear DNA, and the relative mtDNA copy number calculated by normalizing to β-actin gene copy number. The following primer pairs were used: Cytochrome b: 5'-CAT TTA TTA TCG CGG CCC TA-3' and 5'-TGT TGG GTT GTT TGA TCC TG-3'; β-actin: 5'-AGA GGG AAA TCG TGC GTG AC-3' and 5'-CAA TAG TGA TGA CCT GGC CGT-3'.

Mice. C57BL/6 male mice were housed individually at a standard 12-h light/dark cycle at 22°C in a pathogen free animal facility and were used for all experiments. Numbers of mice used in the separate experiments can be retrieved from the figure legends. Single caged mice of 3 months of age were fed ad libitum or fed calorie restricted (70% of normal food intake) for 4 weeks. For the other experiment mice were fed high fat diet or normal control diet (Research Diets Inc., product D12492: 60% Fat, 20% Carbohydrates, 20% protein; control diet D12450B, 10% fat, 70% Carbohydrates, 20% Protein) for 20 weeks. Mice were sacrificed by isoflurane at the end of each study. All animal experiments were performed in compliance with protocols approved by the Institutional Animal Care and Use Committee.

Acknowledgements

We thank Daniel Tenen, SCI Singapore/ Harvard Medical School for providing the anti-Ac-K298-C/EBPα antibody, Tony Kouzarides, Cambridge University, for providing the P/CAF-FLAG expression vector, Junjie Chen, University of Texas, for providing the Tip60 expression vector and Richard Eckner, University of Zurich, for providing the p300-HA, ΔKAT-p300-HA expression vectors. M.A.Z. and T.A. were supported by the Leibniz Graduate School on Ageing and Age-Related Diseases (LGSA; www.fli-leibniz.de/phd/) and the UMCG. G.H. was supported by the LGSA and Deutsche Krebshilfe e.V. through a grant (#110193) to C.F.C.

References

1 Wang, N. D. *et al.* Impaired energy homeostasis in C/EBP alpha knockout mice. *Science* **269**, 1108-1112 (1995).

2 Darlington, G. J., Wang, N. & Hanson, R. W. C/EBP alpha: a critical regulator of genes governing integrative metabolic processes. *Curr Opin Genet Dev* **5**, 565-570 (1995).

3 Croniger, C. *et al.* Role of the isoforms of CCAAT/enhancer-binding protein in the initiation of phosphoenolpyruvate carboxykinase (GTP) gene transcription at birth. *J Biol Chem* **272**, 26306-26312 (1997).

4 Inoue, Y., Inoue, J., Lambert, G., Yim, S. H. & Gonzalez, F. J. Disruption of hepatic C/EBPalpha results in impaired glucose tolerance and age-dependent hepatosteatosis. *J Biol Chem* **279**, 44740-44748, doi:10.1074/jbc.M405177200 (2004).

5 Lee, Y. H., Sauer, B., Johnson, P. F. & Gonzalez, F. J. Disruption of the c/ebp alpha gene in adult mouse liver. *Mol Cell Biol* **17**, 6014-6022 (1997).

6 Yang, J. *et al.* Metabolic response of mice to a postnatal ablation of CCAAT/enhancer-binding protein alpha. *J Biol Chem* **280**, 38689-38699, doi:10.1074/jbc.M503486200 (2005).

7 Lefterova, M. I. *et al.* PPARgamma and C/EBP factors orchestrate adipocyte biology via adjacent binding on a genome-wide scale. *Genes Dev* **22**, 2941-2952, doi:10.1101/gad.1709008 (2008).

8 Rosen, E. D. *et al.* C/EBPalpha induces adipogenesis through PPARgamma: a unified pathway. *Genes Dev* **16**, 22-26, doi:10.1101/gad.948702 (2002).

9 Siersbaek, R. & Mandrup, S. Transcriptional networks controlling adipocyte differentiation. *Cold Spring Harb Symp Quant Biol* **76**, 247-255, doi:10.1101/sqb.2011.76.010512 (2011).

10 Pedersen, T. A. *et al.* Distinct C/EBPalpha motifs regulate lipogenic and gluconeogenic gene expression in vivo. *EMBO J* **26**, 1081-1093, doi:10.1038/sj.emboj.7601563 (2007).

11 Menzies, K. J., Zhang, H., Katsyuba, E. & Auwerx, J. Protein acetylation in metabolism - metabolites and cofactors. *Nat Rev Endocrinol* **12**, 43-60, doi:10.1038/nrendo.2015.181 (2016).

12 Choudhary, C., Weinert, B. T., Nishida, Y., Verdin, E. & Mann, M. The growing landscape of lysine acetylation links metabolism and cell signalling. *Nat Rev Mol Cell Biol* **15**, 536-550, doi:10.1038/nrm3841 (2014).

13 Xiong, Y. & Guan, K. L. Mechanistic insights into the regulation of metabolic enzymes by acetylation. *J Cell Biol* **198**, 155-164, doi:10.1083/jcb.201202056 (2012).

14 Houtkooper, R. H., Pirinen, E. & Auwerx, J. Sirtuins as regulators of metabolism and healthspan. *Nat Rev Mol Cell Biol* **13**, 225-238, doi:10.1038/nrm3293 (2012).

15 Bararia, D. *et al.* Proteomic identification of the MYST domain histone acetyltransferase TIP60 (HTATIP) as a co-activator of the myeloid transcription factor C/EBPalpha. *Leukemia* **22**, 800-807, doi:10.1038/sj.leu.2405101 (2008).

16 Erickson, R. L., Hemati, N., Ross, S. E. & MacDougald, O. A. p300 coactivates the adipogenic transcription factor CCAAT/enhancer-binding protein alpha. *J Biol Chem* **276**, 16348-16355 (2001).

17 Jurado, L. A., Song, S., Roesler, W. J. & Park, E. A. Conserved amino acids within CCAAT enhancer-binding proteins (C/EBP(alpha) and beta) regulate phosphoenolpyruvate

carboxykinase (PEPCK) gene expression. *J Biol Chem* **277**, 27606-27612, doi:10.1074/jbc.M201429200 (2002).

18 Yoshida, Y. *et al.* C/EBPalpha and HNF6 protein complex formation stimulates HNF6-dependent transcription by CBP coactivator recruitment in HepG2 cells. *Hepatology* **43**, 276-286, doi:10.1002/hep.21044 (2006).

19 Shi, L. & Tu, B. P. Acetyl-CoA and the regulation of metabolism: mechanisms and consequences. *Curr Opin Cell Biol* **33**, 125-131, doi:10.1016/j.ceb.2015.02.003 (2015).

20 Sterneck, E., Muller, C., Katz, S. & Leutz, A. Autocrine growth induced by kinase type oncogenes in myeloid cells requires AP-1 and NF-M, a myeloid specific, C/EBP-like factor. *EMBO J* **11**, 115-126 (1992).

21 Verdin, E. & Ott, M. 50 years of protein acetylation: from gene regulation to epigenetics, metabolism and beyond. *Nat Rev Mol Cell Biol* **16**, 258-264, doi:10.1038/nrm3931 (2015).

22 Bararia, D. *et al.* Acetylation of C/EBPalpha inhibits its granulopoietic function. *Nat Commun* **7**, 10968, doi:10.1038/ncomms10968 (2016).

23 Nishida, Y. *et al.* SIRT5 Regulates both Cytosolic and Mitochondrial Protein Malonylation with Glycolysis as a Major Target. *Mol Cell* **59**, 321-332, doi:10.1016/j.molcel.2015.05.022 (2015).

24 Park, J. *et al.* SIRT5-mediated lysine desuccinylation impacts diverse metabolic pathways. *Mol Cell* **50**, 919-930, doi:10.1016/j.molcel.2013.06.001 (2013).

25 Wang, L., Du, Y., Lu, M. & Li, T. ASEB: a web server for KAT-specific acetylation site prediction. *Nucleic Acids Res* **40**, W376-379, doi:10.1093/nar/gks437 (2012).

26 Bartels, M. *et al.* Acetylation of C/EBPepsilon is a prerequisite for terminal neutrophil differentiation. *Blood* **125**, 1782-1792, doi:10.1182/blood-2013-12-543850 (2015).

27 Carmona, M. C. *et al.* Mitochondrial biogenesis and thyroid status maturation in brown fat require CCAAT/enhancer-binding protein alpha. *J Biol Chem* **277**, 21489-21498, doi:10.1074/jbc.M201710200 (2002).

28 Rodgers, J. T. *et al.* Nutrient control of glucose homeostasis through a complex of PGC-1alpha and SIRT1. *Nature* **434**, 113-118, doi:10.1038/nature03354 (2005).

29 Gerhart-Hines, Z. *et al.* Metabolic control of muscle mitochondrial function and fatty acid oxidation through SIRT1/PGC-1alpha. *EMBO J* **26**, 1913-1923, doi:10.1038/sj.emboj.7601633 (2007).

30 Nemoto, S., Fergusson, M. M. & Finkel, T. SIRT1 functionally interacts with the metabolic regulator and transcriptional coactivator PGC-1{alpha}. *J Biol Chem* **280**, 16456-16460, doi:10.1074/jbc.M501485200 (2005).

31 Brunet, A. *et al.* Stress-dependent regulation of FOXO transcription factors by the SIRT1 deacetylase. *Science* **303**, 2011-2015, doi:10.1126/science.1094637 (2004).

32 Motta, M. C. *et al.* Mammalian SIRT1 represses forkhead transcription factors. *Cell* **116**, 551-563 (2004).

33 van der Horst, A. *et al.* FOXO4 is acetylated upon peroxide stress and deacetylated by the longevity protein hSir2(SIRT1). *J Biol Chem* **279**, 28873-28879, doi:10.1074/jbc.M401138200 (2004).

34 Qiao, L. & Shao, J. SIRT1 regulates adiponectin gene expression through Foxo1-C/enhancer-binding protein alpha transcriptional complex. *J Biol Chem* **281**, 39915-39924, doi:10.1074/jbc.M607215200 (2006).

35 Leutz, A., Pless, O., Lappe, M., Dittmar, G. & Kowenz-Leutz, E. Crosstalk between phosphorylation and multi-site arginine/lysine methylation in C/EBPs. *Transcription* **2**, 3-8, doi:10.4161/trns.2.1.13510 (2011).

36 Nerlov, C. C/EBPs: recipients of extracellular signals through proteome modulation. *Curr Opin Cell Biol* **20**, 180-185, doi:10.1016/j.ceb.2008.02.002 (2008).

37 Kim, J., Cantwell, C. A., Johnson, P. F., Pfarr, C. M. & Williams, S. C. Transcriptional activity of CCAAT/enhancer-binding proteins is controlled by a conserved inhibitory domain that is a target for sumoylation. *J Biol Chem* **277**, 38037-38044, doi:10.1074/jbc.M207235200 (2002).

38 Sato, Y., Miyake, K., Kaneoka, H. & Iijima, S. Sumoylation of CCAAT/enhancer-binding protein alpha and its functional roles in hepatocyte differentiation. *J Biol Chem* **281**, 21629-21639, doi:10.1074/jbc.M600852200 (2006).

39 Muller, C., Bremer, A., Schreiber, S., Eichwald, S. & Calkhoven, C. F. Nucleolar retention of a translational C/EBPalpha isoform stimulates rDNA transcription and cell size. *EMBO J* **29**, 897-909, doi:10.1038/emboj.2009.404 (2010).

40 Bordoli, L. *et al.* Functional analysis of the p300 acetyltransferase domain: the PHD finger of p300 but not of CBP is dispensable for enzymatic activity. *Nucleic Acids Res* **29**, 4462-4471 (2001).

41 Reid, J. L., Bannister, A. J., Zegerman, P., Martinez-Balbas, M. A. & Kouzarides, T. E1A directly binds and regulates the P/CAF acetyltransferase. *EMBO J* **17**, 4469-4477, doi:10.1093/emboj/17.15.4469 (1998).

42 Wang, J. & Chen, J. SIRT1 regulates autoacetylation and histone acetyltransferase activity of TIP60. *J Biol Chem* **285**, 11458-11464, doi:10.1074/jbc.M109.087585 (2010).

43 Li, K. *et al.* Regulation of WRN protein cellular localization and enzymatic activities by SIRT1-mediated deacetylation. *J Biol Chem* **283**, 7590-7598, doi:10.1074/jbc.M709707200 (2008).

44 McCarthy, D. J., Chen, Y. & Smyth, G. K. Differential expression analysis of multifactor RNA-Seq experiments with respect to biological variation. *Nucleic Acids Res* **40**, 4288-4297, doi:10.1093/nar/gks042 (2012).

45 Robinson, M. D., McCarthy, D. J. & Smyth, G. K. edgeR: a Bioconductor package for differential expression analysis of digital gene expression data. *Bioinformatics* **26**, 139-140, doi:10.1093/bioinformatics/btp616 (2010).

46 Huang da, W., Sherman, B. T. & Lempicki, R. A. Systematic and integrative analysis of large gene lists using DAVID bioinformatics resources. *Nat Protoc* **4**, 44-57, doi:10.1038/nprot.2008.211 (2009).

Supplementary Figures and Tables

A C/EBPalpha alignment highlighting conserved Lysines

```
RAT      MESADFYEAEPRPPMSSHLQSPPHAPSNA-AFGF-PRGAGPAPPPAPPAAPE  50
HUMAN    MESADFYEAEPRPPMSSHLQSPPHAPSSA-AFGF-PRGAGPPKPPAPPAAPE
COW      MESADFYEAEPRPPMSSHLQSPPHAPSSA-AFGF-PRGAGPSQPPAPPAAPE
CHICKEN  MEQANFYEVDSRPPMSSGQHHQLQTPLPGSAYGYREA-PSAAAPAAGGA--E
         ** * ***    ******         *      *          *       *

                    TAD1

                                                    90/92
RAT      PLGGICEHETSIDISAYIDPAAFNDEFLADLFQHSRQQEKAKAAAGPAGGGG 102
HUMAN    PLGGICEHETSIDISAYIDPAAFNDEFLADLFQHSRQQEKAKAAVGPTGGGG
COW      PLGGICEHETSIDISAYIDPAAFNDEFLADLFQHSRQQEKAKAAAAPAGGG-
CHICKEN  ELGDICENEHSIDISAYIDPAAFNDEFLADLFQHSKQQEKHKAVLAG-----
          ** ***** ************************** ****  **   *

RAT      --DFDYPGAPAGPGGAVMSAGAHGPPPGY--GCAAAGYLDGRLEPLYERVGA 150
HUMAN    GGDFDYPGAPAGPGGAVMPGGAHGPPPGY--GCAAAGYLDGRLEPLYERVGA
COW      -NDFDYPGAPVGPGGAVMPGGTHGPPPGY--GCAAAGYLDSRLEPLYERVGA
CHICKEN  --DFDFHGMHGAGAAASAPGHHPQHQQQPLFGC-AAGYMDGKLDPLYERIAA
           ***  *       *                ** **** *  * *****  *

         TAD2
                159       169
RAT      PALRPLVIKQEPREEDEAKQLALAGLFPYQPPPPPPPPHPHASPA--HLAAP 200
HUMAN    PALRPLVIKQEPREEDEAKQLALAGLFPYQPPPPPPPSHPHPHPPPAHLAAP
COW      PALRPLVIKQEPREEDEAKQLALAGLFPYQPPPPPPPPNSHP--PPAHLAAP
CHICKEN  PGLRPLVIKQEPREEEEVKAAALAALYPHPQQ--------HPS---------
         * *************  * *   *  * *            *

         TAD3
                                                        250
RAT      HLQFQIAHCGQTTMHLQPGHPTPPPTPVPSPHPAPAMGAAG-LPGPGGSLKG 251
HUMAN    HLQFQIAHCGQTTMHLQPGHPTPPPTPVPSPHPAPALGAAG-LPGPGSALKG
COW      HLQFQIAHCGQTTMHLQPGHPTPPPTPVPSPHPAPALGAAG-LPGPGGALKG
CHICKEN  HLQYQIAHCAQTTVHLQPGHPTPPPTPVPSPHHPHHPHPPGALPAAPGALKM
         ********* *** ******************        * **   * **

                                          DBD
                          273/275/276/280          298/302
RAT      LAGPHPDLRTGGGGGGGAGAGKAKKSVDKNSNEYRVRRERNNIAVRKSRDKA 303
HUMAN    LGAAHPDLRASGGT----GAGKAKKSVDKNSNEYRVRRERNNIAVRKSRDKA
COW      LVATHPDLRAGGG-----GGGKAKKSVDKNSNEYRVRRERNNIAVRKSRDKA
CHICKEN  MPA---DHR----------GKSKKTVDKNSNEYRVRRERNNIAVRKSRDKA
               * *           ** ** **********************_*****

         LZIP
         304      313          326                       352
RAT      KQRNVETQQKVLELTSDNDRLRKRVEQLSRELDTLRGIFRQLPESSLVKAMG 355
HUMAN    KQRNVETQQKVLELTSDNDRLRKRVEQLSRELDTLRGIFRQLPESSLVKAMG
COW      KQRNVETQQKVLELTSDNDRLRKRVEQLSRELDTLRGIFRQLPESSLVKAMG
CHICKEN  KQRNVETQQKVLELTTDNERLRKRVEQLSRELETLRGIFRQLPESSLVKAMG
         ********** ****** ********** ****************_***

RAT      NCA 358
HUMAN    NCA
COW      NCA
CHICKEN  SCA
         ***
```

B

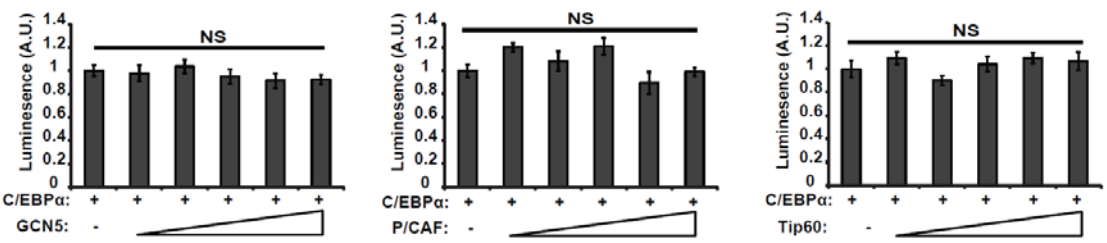

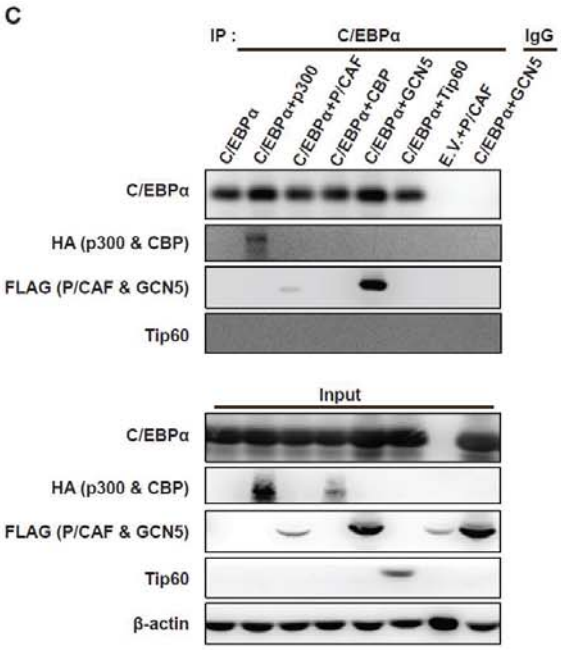
C
IP :
C/EBPα
IgG
C/EBPα
C/EBPα+p300
C/EBPα+P/CAF
C/EBPα+CBP
C/EBPα+GCN5
C/EBPα+Tip60
E.V.+P/CAF
C/EBPα+GCN5
C/EBPα
HA (p300 & CBP)
FLAG (P/CAF & GCN5)
Tip60
Input
C/EBPα
HA (p300 & CBP)
FLAG (P/CAF & GCN5)
Tip60
β-actin

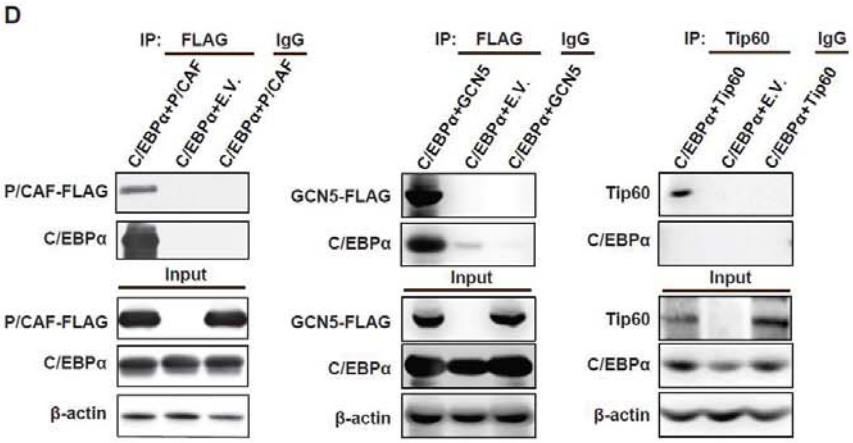
D
IP: FLAG
IgG
C/EBPα+P/CAF
C/EBPα+E.V.
C/EBPα+P/CAF
P/CAF-FLAG
C/EBPα
Input
P/CAF-FLAG
C/EBPα
β-actin
IP: FLAG
IgG
C/EBPα+GCN5
C/EBPα+E.V.
C/EBPα+GCN5
GCN5-FLAG
C/EBPα
Input
GCN5-FLAG
C/EBPα
β-actin
IP: Tip60
IgG
C/EBPα+Tip60
C/EBPα+E.V.
C/EBPα+Tip60
Tip60
C/EBPα
Input
Tip60
C/EBPα
β-actin

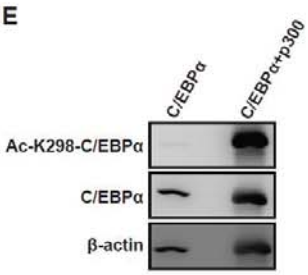
E
C/EBPα
C/EBPα+p300
Ac-K298-C/EBPα
C/EBPα
β-actin

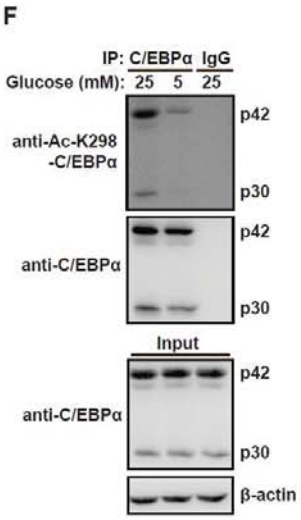
F
IP: C/EBPα
IgG
Glucose (mM): 25 5 25
anti-Ac-K298 -C/EBPα
p42
p30
anti-C/EBPα
p42
p30
Input
anti-C/EBPα
p42
p30
β-actin

Supplementary Figure 1.

(**A**) Alignment of four different C/EBPα vertebrate orthologs with the conserved lysines numbered and colored in red. TAD: transactivation domain, DBD: DNA binding domain and LZIP: leucine zipper domain.

(**B**) HEK293T cells were transiently transfected with luciferase C/EBPα responsive promoter vector, renilla expression vector for normalization, C/EBPα expression vector and increased amounts of either GCN5, P/CAF or Tip60 expression vectors. Luciferase activity was measured 48 h later (n=3). Statistical differences were analyzed by Student's t-tests. Error bars represent ±SD, *P<0.05, **P<0.01, ***P<0. 001. NS: not significant.

(**C**) HEK293T cells were cotransfected with C/EBPα and one of the lysine acetyl transferases (KATs) p300-HA, P/CAF-FLAG, CBP-HA, GCN5-FLAG or Tip60 expression vectors as indicated. Cell lysates were immunoprecipitated with rabbit anti-C/EBPα antibody or with rabbit IgG as control followed by immunoblotting. Immunoblots of immunoprecipitates (IP) and total lysates (Input) were stained as indicated.

(**D**) HEK293T cells were cotransfected with C/EBPα and either pcDNA3 empty vector (E.V.), P/CAF-FLAG, GCN5-FLAG or Tip60 expression vectors. Cell lysates were immunoprecipitated with mouse anti-FLAG antibody and mouse IgG as control (first two panels) or with rabbit anti-Tip60 antibody and rabbit IgG as control (third panel) followed by immunoblotting. Immunoblots of immunoprecipitates (IP) and total lysates (Input) were stained as indicated. Mouse or rabbit IgG antibodies were used as IP loading control.

(**E**) HEK293T cells were cotransfected with C/EBPα alone or with C/EBPα and p300-HA expression vectors. Total cell lysates were analyzed by immunoblotting for acetylated-K298-C/EBPα, C/EBPα or β-actin loading control as indicated.

(**F**) Immunoprecipitation (IP) of endogenous C/EBPα was performed with rabbit anti-C/EBPα antibody or with rabbit IgG as control from total lysates of Fao cells cultured overnight in either high (25 mM) or low (5 mM) glucose medium. The immunoprecipitates (IP) and total lysates (Input) were analyzed by immunoblotting for acetylated-K298-C/EBPα, C/EBPα or β-actin loading control as indicated.

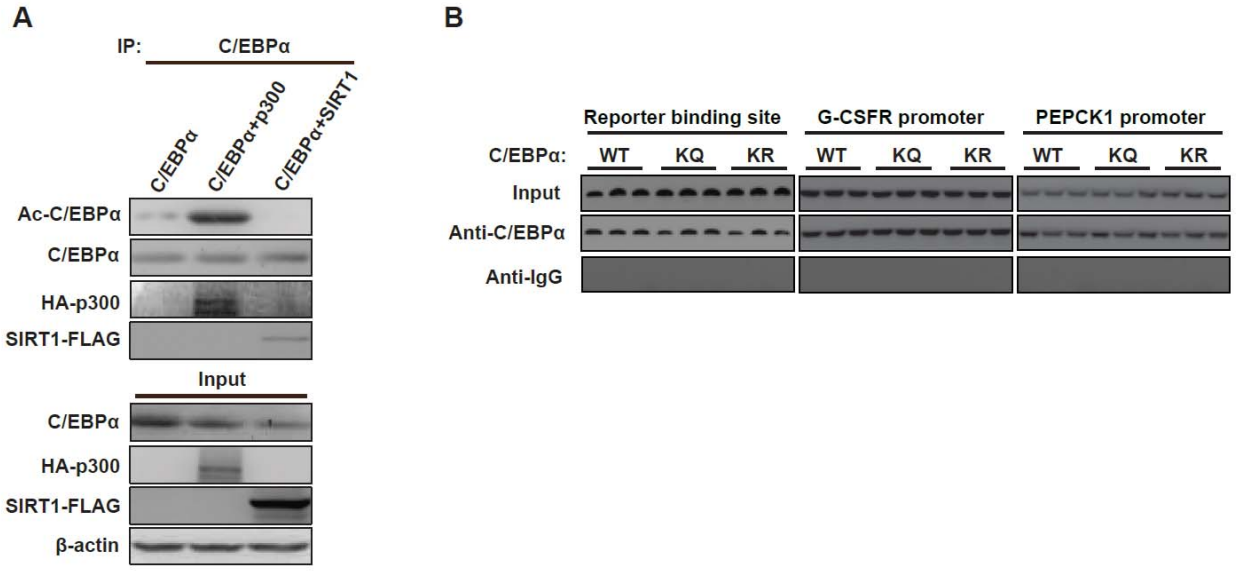

Supplementary Figure 2.

(A) HEK293T cells were cotransfected with either C/EBPα alone, C/EBPα with p300-HA or C/EBPα with SIRT1-FLAG expression vectors. Cell lysates were immunoprecipitated with rabbit anti-C/EBPα antibody followed by immunoblotting. Immunoblots of immunoprecipitates (IP) and total lysates (Input) were stained as indicated. Rabbit IgG antibody was used as IP loading control.

(B) DNA gel of semi-quantitative PCR with input and DNA immunoprecipitation or ChIP assays with anti-C/EBPα or IgG antibodies performed in (Figures 4G and H).

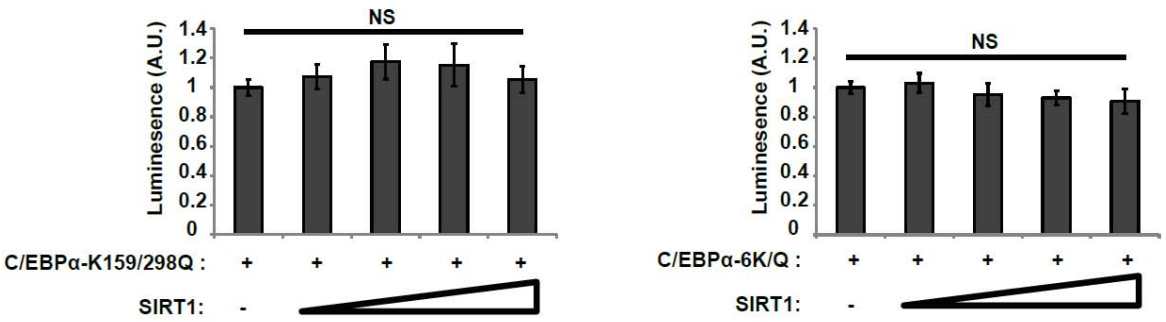

Supplementary Figure 3.

HEK293T cells were transiently transfected with luciferase C/EBPα responsive promoter vector, renilla expression vector for normalization, increased amounts of SIRT1and either K159/298Q mutated C/EBPα (left panel) or 6K/Q mutated C/EBPα expression vectors. Luciferase activity was measured 48 h later (n=3). Statistical differences were analyzed by Student's t-tests. Error bars represent ±SD, *P<0.05, **P<0.01, ***P<0. 001. NS: not significant.

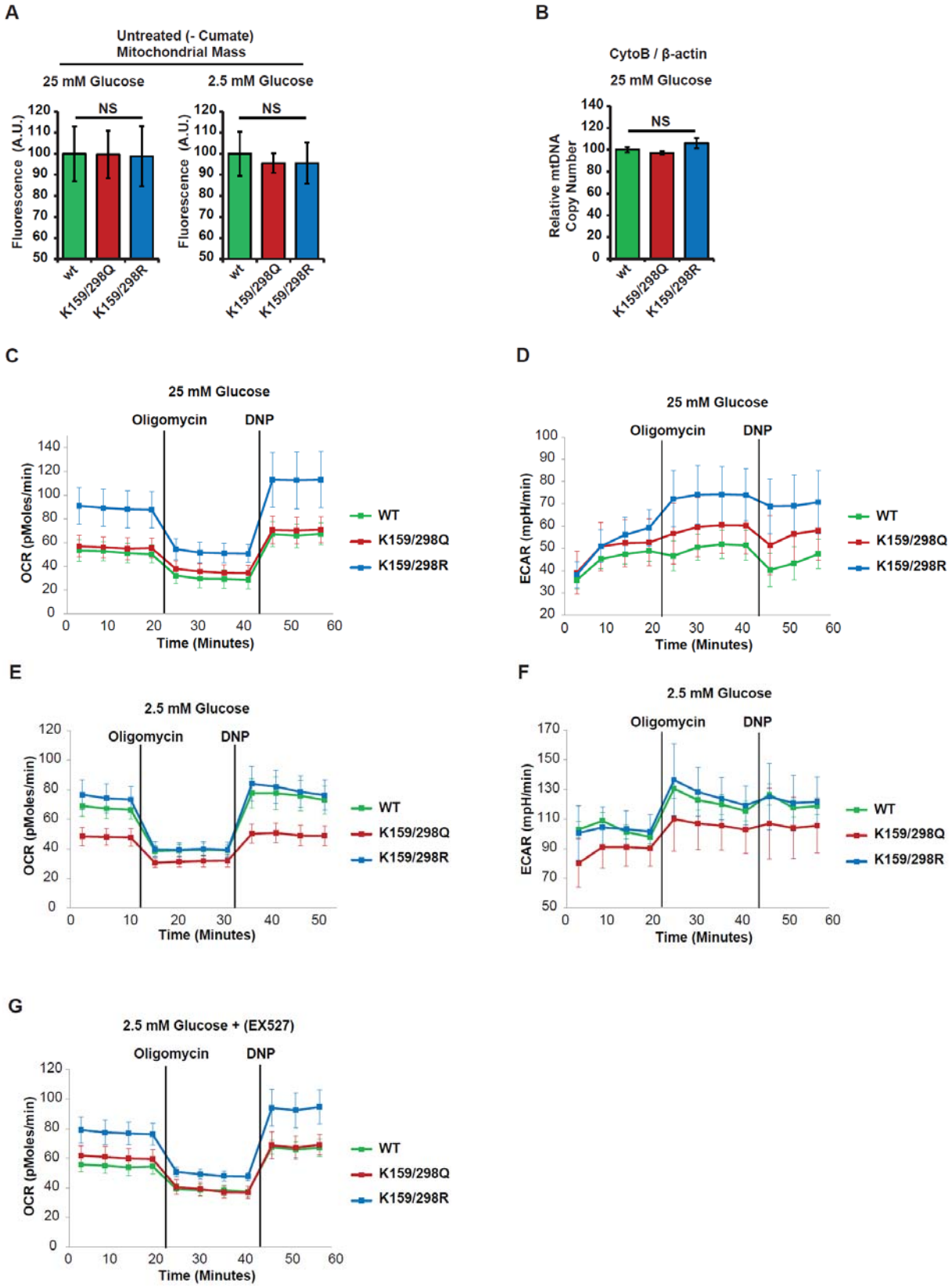

Supplementary Figure 4.

(**A**) Mitochondrial mass measured by MitoTracker fluorescent dye in untreated (- Cumate) Hepa1-6 cells which were used in Figure 7A (n=5).

(**B**) Relative mtDNA copy number of cumate-induced Hepa1-6 cells expressing wt-, K159/298Q- or K159/298R-C/EBPα-FLAG and cultured in 25 mM glucose medium. mtDNA copy number was calculated by qRT-PCR of the mitochondrial cytochrome b gene and the nuclear β-actin gene. Presented is the ratio of the copy number in cells. (n=3). Statistical differences were analyzed by Student's t-tests. Error bars represent ±SD, *P<0.05, **P<0.01, ***P<0. 001. NS: not significant. mtDNA: mitochondrial DNA.

(**C**), (**E**) and (**G**) Oxygen consumption rate (OCR) traces in cumate-induced Hepa1-6 cells expressing wt-, K159/298Q- or K159/298R-C/EBPα-FLAG proteins and cultured in medium with 25 mM glucose (C), 2.5 mM glucose (E) or 2.5 mM glucose and treated with the SIRT1 inhibitor Ex-527 (Selisistat) 16 hours before the measurement (G). Values are means ± SE, (n = 5).

(**D**) and (**F**) Extra-cellular acidification rate (ECAR) traces in cumate-induced Hepa1-6 cells expressing wt-, K159/298Q- or K159/298R-C/EBPα-FLAG proteins and cultured in medium with 25 mM glucose (D) or 2.5 mM glucose (F). Values are means ± SE, (n = 5).

Supplementary Table 1

Lysine position	MasSpec identified Acetylation	LAceP predicted p300 KAT	ASEB predicted Sirt1 KDAC
90	NC	No (0.108)	No (p=0.4795)
92	No	No (0.275)	No (p=0.1318)
159	**Yes**	No (0.156)	**Yes (p=0.0167)**
169	No	No (0.014)	No (p=0.9382)
250	**Yes**	**Yes (0.539)**	**Yes (p=0.0258)**
273	**Yes**	**Yes (0.992)**	**Yes (p=0.0003)**
275	**Yes**	**Yes (0.672)**	**Yes (p=0.0210)**
276	**Yes**	**Yes (0.640)**	**Yes (p=0.0009)**
280	No	**Yes (0.955)**	**Yes (p=0.0361)**
298	NC	**Yes (0.723)**	**Yes (p=0.0052)**
302	NC	No (0.173)	No (p=0.5452)
304	No	No (0.138)	No (p=0.0889)
313	No	No (0.158)	No (p=0.4970)
326	NC	No (0.027)	No (p=0.1942)
352	No	No (0.016)	No (p=0.9647)

NC is not covered

ASAB: A lower P-value indicates a higher probability of acetylation by the selected KAT family. The background P-values were calculated from all lysine sites on human proteins and then ranked from lowest to highest. Lysine sites with P-values lower than the top 10% are in red.

Supplementary Table 2

Upregulated genes (Oxidation reduction process) P-value=0.0006						
DAVID List ID	**Gene Name**	**Cluster Score (out of 1000)**	**Layered H3K27AC**	**Rel. to start site/locus**	**C/EBPβ site position**	**Cell line**
11532	alcohol dehydrogenase 5 (class III), chi polypeptide(Adh5)	940	Yes	+587	chr4:100009264-100009587	Af49 HeLa-S3 HepG2 IMR90 K562
11668	aldehyde dehydrogenase family 1, subfamily A1(Aldh1a1)	507	Yes	-1794	chr9:75570027-75570282	A549
		518	Yes	-1312	chr9:75569545-75569800	A549
13076	cytochrome P450, family 1, subfamily a, polypeptide 1(Cyp1a1)	246	No	-10439	chr15:75027665-75027888	HepG2
		324	No	-8842	chr15:75024280-75024543	HeLa-S3
		135	No	-7831	chr15:75023269-75023492	HepG2
13086	cytochrome P450, family 2, subfamily a, polypeptide 4(Cyp2a4)	No site				
13113	cytochrome P450, family 3, subfamily a, polypeptide 13(Cyp3a13)					
15926	isocitrate dehydrogenase 1 (NADP+), soluble(Idh1)	1000	Yes	+2123	chr2:20917683-209117938	HeLa-S3 HepG2 IMR90 K562
		195	Yes	+1667	chr2:20918139-209118402	HeLa-S3 HepG2
		1000	Yes	+977	chr2:20918829-209119098	A549 H1-hESC HeLa-S3 HepG2 IMR90 K562
		181	Yes	-133	chr2:20919939-209120202	HeLa-S3
18484	peptidylglycine alpha-amidating monooxygenase(Pam)	201	No	-6661	chr5:102194611-102194866	IMR90
		206	Yes	-436		IMR90
		516	Yes	+73	chr5:102200836-102201091	HeLa-S3 IMR90
					chr5:102201319-102201600	
11757	peroxiredoxin 3(Prdx3)	201	Yes	-25	chr10:120938320-120938583	HeLa-S3
		202	No	-4846	chr10:120943209-120943464	HepG2 IMR90
69051	pyrroline-5-carboxylate reductase family, member 2(Pycr2)	392	Yes	-4445	chr1:226116162-22611648	K562

		1000	Yes	+212	5 chr1:226111828-226112091	A549 H1-hESC HeLa-S3 HepG2 IMR90 K562
98711	retinol dehydrogenase 10 (all-trans) (Rdh10)	202	Yes	-769	chr8:74205553-74206068	GM12878
59010	sulfide quinone reductase-like (yeast) (Sqrdl)	1000	Yes	+100	chr15:45926781-45927038	A549 HeLa-S3 HepG2

Up regulated genes (Mitochonderion) P-Value=0.0008						
DAVID List ID	**Gene Name**	**Cluster Score (out of 1000)**	**Layered H3K27AC**	**Rel. to start site/locus**	**C/EBPβ site position**	**Cell line**
11950	ATP synthase, H+ transporting, mitochondrial F0 complex, subunit B1(Atp5f1)	251	No	-9414	chr1:111991774-111992045	K562
		251	Yes	+302	chr1:111982329-111982604	HeLa-S3 IMR90
14373	G0/G1 switch gene 2(G0s2)	192	No	-7886	chr1:209840461-209840784	K562
		1000	Yes	-4342	chr1:209844143-209844328	HeLa-S3
		1000	Yes	-117	chr1:209847285-209847553	A549, H1-hESC, HeLa-S3 HepG2 IMR90 K562
		267	Yes	-1694	chr1:209846713-209846976	HeLa-S3
65102	Ngg1 interacting factor 3-like 1 (S. pombe) (Nif3l1)	384	Yes	+2574	chr2:201753830-201754093	HeLa-S3
		371	Yes	+1849	chr2:201754098-201754818	K562 GM12878
74205	acyl-CoA synthetase long-chain family member 3(Acsl3)	818	No	-8435	chr2:223716974-223717297	H1-hESC HeLa-S3 HepG2 IMR90 K562
		430	Yes	-836	chr2:223724633-223724896	HeLa-S3 HepG2
11532	alcohol dehydrogenase 5 (class III), chi polypeptide(Adh5)	940	Yes	+587	chr4:100009264-100009587	Af49 HeLa-S3 HepG2 IMR90 K562
13076	cytochrome P450, family 1, subfamily a, polypeptide 1(Cyp1a1)	246	No	-10439	chr15:75027665-75027888	HepG2

					8	
		324	No	-8842	chr15:75024280-75024543	HeLa-S3
		135	No	-7831	chr15:75023269-75023492	HepG2
15528	heat shock protein 1 (chaperonin 10) (Hspe1)	218	Yes	+126	chr2:198364581-198364847	HepG2
		624	Yes	-1408	chr2:198363058-198363313	HeLa-S3 IMR90
15926	isocitrate dehydrogenase 1 (NADP+), soluble(Idh1)	1000	Yes	+2123	chr2:209117683-209117938	HeLa-S3 HepG2 IMR90 K562
		195	Yes	+1667	chr2:209118139-209118402	HeLa-S3 HepG2
		1000	Yes	+977	chr2:209118829-209119098	A549 H1-hESC HeLa-S3 HepG2 IMR90 K562
		181	Yes	-133	chr2:209119939-209120202	HeLa-S3
27395	mitochondrial ribosomal protein L15(Mrpl15)	962	Yes	-196	chr8:55047260-55047585	HeLa-S3 HepG2 IMR90 K562
107734	mitochondrial ribosomal protein L30(Mrpl30)	371	Yes	+513	chr2:99797369-99798055	GM12878 HeLa-S3 HepG2 IMR90 K562
		353	No	-3323	chr2:99793940-99794219	A549 HepG2 IMR90
78523	mitochondrial ribosomal protein L9(Mrpl9)	216	Yes	-10217	chr1:151746257-151746520	HeLa-S3
11757	peroxiredoxin 3(Prdx3)	202	No	-4869	chr10:120943209-120943464	HepG2 IMR90
		201	Yes	-25	chr10:120938320-120938583	HeLa-S3
74776	pyrophosphatase (inorganic) 2(Ppa2)	No site				
69051	pyrroline-5-carboxylate reductase family, member 2(Pycr2)	392	Yes	-4445	chr1:226116162-226116485	K562
		1000	Yes	+212	chr1:226111828-226112091	A549 H1-hESC HeLa-S3 HepG2 IMR90

						K562
67223	ribosomal RNA processing 15 homolog (S. cerevisiae)(Rrp15)	254	Yes	+240	chr1:218458354-218458869	GM12878
20044	ribosomal protein S14(Rps14)	No site				
109552	sorcin(Sri)	205	Yes	-109	chr7:87849589-87850104	GM12878
		189	No	-4513	chr7:87853912-87854175	HeLa-S3
		243	No	-6178	chr7:87855577-87855840	HeLa-S3
		1000	No	-6826	chr7:87856225-87856519	A549 HeLa-S3 HepG2 IMR90
68002	succinate dehydrogenase complex assembly factor 4(Sdhaf4)					
59010	sulfide quinone reductase-like (yeast)(Sqrdl)	1000	Yes	+100	chr15:45926781-45927038	A549 HeLa-S3 HepG2
21854	translocase of inner mitochondrial membrane 17a(Timm17a)	257	Yes	-216	chr1:201924403-201924666	HeLa-S3
		751	No	-7667	chr1:201916594-201916721	IMR90
		215	No	-2217	chr1:201922402-201922677	K562
Up regulated genes (Ribosome) P-Value=0.009						
DAVID List ID	**Gene Name**	**Cluster Score (out of 1000)**	**Layered H3K27AC**	**Rel. to start site/locus**	**C/EBPβ site position**	**Cell line**
27395	mitochondrial ribosomal protein L15(Mrpl15)	962	Yes	-196	chr8:55047260-55047585	HeLa-S3 HepG2 IMR90 K562
107734	mitochondrial ribosomal protein L30(Mrpl30)	371	Yes	+513	chr2:99797369-99798055	GM12878 HeLa-S3 HepG2 IMR90 K562
		353	No	-3323	chr2:99793940-99794219	A549 HepG2 IMR90
78523	mitochondrial ribosomal protein L9(Mrpl9)	216	Yes	-10217	chr1:151746257-151746520	HeLa-S3
114641	ribosomal protein L31(Rpl31)	1000	Yes	+129	chr2:101618497-101618820	A549 H1-hESC HeLa-S3 HepG2 IMR90 K562
20044	ribosomal protein S14(Rps14)	No site				
Downregulated genes (glycoprotein) P-Value=0.0004						
DAVID List ID	**Gene Name**	**Cluster Score**	**Layered H3K27AC**	**Rel. to start**	**C/EBPβ site**	**Cell line**

		(out of 1000)		site/locus	position	
67729	MANSC domain containing 1(Mansc1)	746	Yes	-7021	chr12:12509867-12510190	A549 H1-hESC HeLa-S3 IMR90 HepG2 K562
		568	Yes	-1226	chr12:12504036-12504395	HepG2
100043899	R3H domain containing-like(R3hdml)	186	No	+98	chr20:42965641-42965896	A549 HepG2
		195	No	-899	chr20:42964673-42964899	HepG2
21356	TAP binding protein(Tapbp)	249	Yes	-202	chr6:33282366-33282641	K562
		1000	Yes	-5947	chr6:33288111-33288434	HeLa-S3 IMR90 K562
11803	amyloid beta (A4) precursor-like protein 1(Aplp1)	No site				
382014	anoctamin 8(Ano8)	1000	No	-6059	chr19:17451697-17451964	H1-hESC HeLa-S3 HepG2
		235	Yes	+95	chr19:17445543-17445848	HeLa-S3 K562
100503659	calcium channel, voltage-dependent, beta subunit associated regulatory protein(Cbarp)	1000	Yes	-6457	chr19:1244447-1244777	A549 HeLa-S3 HepG2 IMR90 K562
		258	Yes	-6944	chr19:1244934-1245183	HepG2
		268	Yes	-2964	chr19:1240954-1241229	HepG2 IMR90 K562
		200	Yes	-3570	chr19:1241560-1241823	HeLa-S3
227231	carbamoyl-phosphate synthetase 1(Cps1)	1000	No	0	chr2:211421117-211421323	HeLa-S3
		426	No	-9827	chr2:211411228-211411496	H1-hESC HeLa-S3 HepG2
		1000	No	-7267	chr2:211413721-211414056	A549 HeLa-S3 HepG2
70574	carboxypeptidase M(Cpm)	175	No	-4020	chr12:6933099-69331262	HeLa-S3
		100	No	-6345	chr12:6933324-69333587	A549 HeLa-S3 HepG2
		715	No	+548	chr12:6926431-69326563	HepG2
13039	cathepsin L(Ctsl)					
11443	cholinergic receptor, nicotinic, beta polypeptide 1 (muscle)(Chrnb1)	319	Yes	+424	chr17:7348580-7348830	HepG2

		248	Yes	-7786	chr17:73400357-7340620	HeLa-S3
		349	No	-9894	chr17:73381137-7338512	A549 HeLa-S3 HepG2 IMR90 K562
67896	coiled-coil domain containing 80(Ccdc80)	985	Yes	+911	chr3:112359066-112359329	A549 HeLa-S3 IMR90
		1000	Yes	-5992	chr3:112365969-112366240	A549 H1-hESC HeLa-S3 HepG2 IMR90
12833	collagen, type VI, alpha 1(Col6a1)	No site				
12815	collagen, type XI, alpha 2(Col11a2)	No site				
12931	cytokine receptor-like factor 1(Crlf1)	No site				
12305	discoidin domain receptor family, member 1(Ddr1)	170	Yes	-1302	chr6:30854888-30855163	K562
71522	gamma-glutamyltransferase 6(Ggt6)	No site				
14561	growth differentiation factor 11(Gdf11)	196	Yes	+435	chr12:56137236-56137499	HeLa-S3
		187	No	-9086	chr12:56127703-56127978	K562
23886	growth differentiation factor 15(Gdf15)	313	Yes	-5786	chr19:18490919-18491182	HeLa-S3 HepG2
		160	No	-2657	chr19:18494088-18494311	HepG2
		295	Yes	+308	chr19:18496905-18497276	HeLa-S3 HepG2 K562
192897	integrin beta 4(Itgb4)	300	No	-8546	chr17:73708676-73708970	A549 IMR90
16180	interleukin 1 receptor accessory protein(Il1rap)	312	No	-4071	chr3:190227511-190227769	A549 IMR90 HepG2
		1000	Yes	-276	chr3:190231267-190231564	A549 H1-hESC HeLa-S3 HepG2 IMR90
53978	lysophosphatidic acid receptor 2(Lpar2)	1000	Yes	-711	chr19:19739750-19740006	HeLa-S3 IMR90
103534	mannoside acetylglucosaminyltransferase 4, isoenzyme B(Mgat4b)	381	No	-1378	chr5:179235330-179235632	A549 HeLa-S3
216856	neuroligin 2(Nlgn2)	203	Yes	-3715	chr17:7307414-7307787	A549 HeLa-S3
18073	nidogen 1(Nid1)	211	Yes	-2718	chr1:236231199-236231454	IMR90
		171	No	-9124	chr1:236237605-236237828	HepG2
		568	No	-9604	chr1:236238085-23623834	HeLa-S3 HepG2

					8	
18591	platelet derived growth factor, B polypeptide(Pdgfb)	413	Yes	-8540	chr22:39649497-39649760	HeLa-S3
18846	plexin A3(Plxna3)	No site				
235611	plexin B1(Plxnb1)	1000	Yes	-593	chr3:48471465-48471720	A549 H1-hESC HeLa-S3 HepG2 IMR90 K562
		279	Yes	-2804	chr3:48473676-48473906	HepG2
		208	Yes	-6320	chr3:48477192-48477467	K562
19216	prostaglandin E receptor 1 (subtype EP1) (Ptger1)	1000	Yes	-4211	chr19:14587489-14587812	A549 H1-hESC HeLa-S3 HepG2 IMR90 K562
		839	No	-9733	chr19:14593011-14593334	HeLa-S3 HepG2 IMR90 K562
70835	protease, serine 22(Prss22)	275	Yes	-327	chr16:2908498-2908761	HeLa-S3
56554	retinoic acid early transcript delta(Raet1d)					
20361	sema domain, immunoglobulin domain (Ig), and GPI membrane anchor, (semaphorin) 7A(Sema7a)	274	No	-9638	chr15:74735937-74736194	HepG2
		177	No	-7681	chr15:74733980-74734203	HepG2
		222	No	-4811	chr15:74731110-74731373	HeLa-S3
83704	solute carrier family 12 (potassium/chloride transporters), member 9(Slc12a9)	No site				
69354	solute carrier family 38, member 4 (Slc38a4)	No site				
232086	transmembrane protein 150A(Tmem150a)	260	Yes	-3198	chr2:85833020-85833275	IMR90
		412	Yes	-2662	chr2:85832209-85832484	HepG2 IMR90 K562
		227	Yes	-28	chr2:85829850-85830095	HepG2
72309	transmembrane protein 158(Tmem158)	310	No	-1672	chr3:45269486-45269780	H1-hESC K562
94185	tumor necrosis factor receptor superfamily, member 21(Tnfrsf21)	501	Yes	-72	chr6:47277608-47277871	HepG2 HeLa-S3
78339	tweety family member 3(Ttyh3)	253	No	-8416	chr7:2662964-2663187	HepG2
		224	Yes	-6600	chr7:2664748-2665003	IMR90
		395	Yes	-100	chr7:2671180-2671503	A549 HeLa-S3 HepG2 IMR90 K562

Supplementary Table 3

Gene	Forward 5' to 3'	Reverse 5' to 3'
Aldh1a1	GGCACAATTCAGTGAGCGGC	ATGGTGCGCCATGGAGAGC
Cyp3a13	CCAACCTTCACCAGTGGGAGG	GATCACATCCATGCTGTAGGCCC
Pam	CTGTCAACACTGTTATACCCCCAGG	TCCAATCAGCGTCCACTGTCCG
Prdx3	GCTCTGGTCCTCGGTTGCTCG	GGGTGACAGCAGGGGTGTGG
Pycr2	ATGCTGCTGGACTCAGAGGACC	TTCTTGGTCAGCCATGGACTGC
Rdh10	CCATGATGGTCAACTGCCACGC	GCTCATGGCTCAGAGACTCGTGA
Atp5f1	TGGTATTACAGGCAACAAGGGCC	TCCAGTTCCAAGCACATAAGGTCC
Hspe1	AAGGAAAGAGTGGAGAGATTGAGCC	GAATGGCAGCTTCACGTGACACC
Sdhaf4	GCCCTTAAGAAGTCAAAGCTGCC	CTTCCGTTCCCAGTCTCCATATCG
Timm17a	GCGAATTGTAGATGACTGTGGCGG	GTCAAACTTCCTCGGAGTCTGTGG
Mansc1	CTCAGGAAGACTGTATCGGTGCC	TGTAGGTCACAAGGCCCTTGGC
R3hdml	CGGGACATGAGCGCTTTACTGG	CCACGTACTTCATCAGCTGTGAGG
Ano8	GGCATGGATGAAGACAGTGCCC	CAAAGAAGGCATAGGCACGCG
Cps1	GGGTCAATGGCTGCAGGAGG	CCACAAAATCCACAGACTGGCC
Cpm	CCTGTGGGTTCTCGTTGTGGG	ATGCGTGATTTCCGGGTCTTTCC
Ccdc80	GTCAGTGGCCGACCTGTTGG	CCACAGAGATCCTCCTGGTGGC
Crlf1	GGCTCCTGCCTCTATGTTGGC	ATGTGTTATCCTGACCGTACCACC
Gdf15	CCTGAGTCCCAACTCAACGCC	CGTGGGACCCCAATCTCACC
Tnfrsf21	CACCGACGCAATGATGTTGTGG	TCACGTTAGGACTGGGCATGG
Plxnb1	TGGGCTGTCTTCGAGTGGTGG	CCAGAACTGGTCAGTAGAGCAGG